AE - 4800: Senior Design Project

Design, Optimization, and Construction of
Flexure, Optical, Damping, and Leveling Systems
for Electric Propulsion Thrust Stand

Nathaniel Allwine
Jeremy Baiocchi
Logan Hefferan

Group Number: 04-22-13

Department of Mechanical and Aerospace Engineering
Western Michigan University
19th April 2022

Disclaimer

This project report was written by students at Western Michigan University to fulfill an engineering curriculum requirement. Western Michigan University makes no representation that the material contained in this report is error-free or complete in all respects. Persons or organizations who choose to use this material do so at their own risk.

Design, Optimization, and Construction of Flexure, Optical, Damping, and Leveling Systems for Electric Propulsion Thrust Stand

An Thrust Stand is a device that uses the basic principles of torsion and displacement to experimentally measure and calculate the thrust generated by an Electric Propulsion (EP) Thruster. Western Michigan University is host to three organizations that work with electric propulsion thrusters currently without a way of obtaining direct experimental thrust data. For this Senior Design Project, the flexure, optical sensing, damping and leveling systems for a thrust stand originally designed by Hannah Watts in her WMU Honors Thesis: Design of A Thrust Stand for Electric Propulsion [13] will be constructed. The four subsystems will be redesigned, optimized, and integrated into the thrust stand for use by student organizations. Additionally, substantial documentation will provided to allow for future reconfiguration, ease of use, and easy replication.

The thrust stand will be operated inside WMU's Aerospace Laboratory for Plasma Experiments (ALPE) large vacuum chamber at pressures ranging from (10^{-7} - 10^{-3} Torr). A modular design will be used to allow for the different organizations to share the same thrust stand. Accuracy, compatibility, size, cost, and the vacuum environment will drive the design criteria for each unique subsystem. Goals for design, construction, and implementation of the various subsystems will be discussed. The proposed thrust measurement range: $10\mu N$ to $1mN$. Ideal measurement accuracy for the thrust stand is $10\mu N$. The estimated budget for construction of the four subsystems is estimated at $5,296.33 USD.

Contents

List of Figures

List of Tables

Chapter 1

Introduction

1.1 Background

1.1.1 Propulsion

With todays technology there are two major leaders in propulsion technology for spacecraft. There are chemical propulsion rockets that use a propellant and oxidizer that combine and form a chemical reaction to combust the propellant and produce thrust. Thrust is the force that is supplied to the spacecraft for maneuvers. This method produces high amounts of thrust at levels around 10^7 Newtons and currently the only viable method to actually reaching space, but not a good choice for long distance space mission. This method is very inefficient with the necessity for high amounts of both the propellant and oxidizer along with complex feed systems. A main limitation of chemical propulsion is the low specific impulse values (I_{sp}) which is the ratio of thrust produced to mass of propellant needed per unit of propellant weight flow. Because of this I_{sp} is measure in units of seconds. Chemical rockets I_{sp} can range from 150 (s) for monopropellants rockets to 450 (s) for bipropellant rockets.

The other leader in spacecraft propulsion is electric propulsion (EP). EP uses a power system and some form of propellant to generate thrust. EP has higher I_{SP} than normal chemical rockets, however, they produce very little thrust. Most EP technologies are still in there infant stage with large inconsistencies and optimization to still be worked out. There are many different EP technologies all of which can be used for different sorts of mission. EP can be separated itself into three categories: electrothermal, electromagnetic and electrostatic. Electrothermal systems heat a gas to be accelerated through a nozzle. Electromagnetic thrusters, on the other hand, use electric and magnetic fields to accelerate a plasma. Lastly, electrostatic system uses magnetic fields to create a plasma which then gets electrostatically accelerated. As previously mentioned, EP thrusters produce very little thrust and can range from 10^1 to as low as 10^{-6} Newtons. Additionally, EP I_{sp} can range from 50 (s) with cold gas thrusters all the way to 3600 (s) with ion thrusters.

Thrust is an important parameter for characterizing propulsion devices since it can be used as a direct comparison and goes into many derived values for comparison such as I_{sp}, thrust-to-weight ratio, and other efficiency parameters. For this reason,

it is a vital value to experimentally gather. [**4**][**6**][**15**]

1.1.2 Thrust Measurement

Since thrust is such a significant value to obtain, strides have been made to acquire very high accuracy readings. Large scale chemical rockets can be place within a sturdy stand and thrust can be measured directly with the use of a load cell. Load cells are a form of transducer that will convert a force to an electrical signal. The basic form of a load cell is that a strain gauge is placed on a metal structure that acts as a spring element. When a force is applied to the load cell, the strain gauge would obtain a measurement. Since chemical rockets are heavier and produce much more thrust than EP, the use of a load cell is adequate for accurate results.

Because of the significantly lower thrust compared to chemical rockets and generally higher thrust-to-weight ratios, EP devices are more difficult to accurately measure thrust. A more advanced system must be used, which in spirit, is similar to that of a load cell. For EP measurements a thrust stand is used which will have a pendulum arm, with the thruster attached at one end and a displacement measurement system at the other. Additionally, thrust stands also will include a form of dampening and calibration. The three most common thrust stand configurations are the torsional pendulum, hanging pendulum and inverted pendulum.

Torsional Pendulum Thrust Stand

A torsional pendulum thrust houses a long pendulum arm that is parallel to the base plate or perpendicular to the gravity vector. The arm rotates about a pivot point and holds the thruster, displacement sensing, damping, and counterweight systems. Other components that are placed on other areas of the stand are the leveling system and calibration system. With the horizontal arm configuration, the effect of gravity can be removed from calculations. This simplifies some of the math, however, a counterweight is added to offset the thruster weight. Since the system is a large pendulum, the sensitivity of the system will mostly be determined by the length of the arm to the thruster, creating a moment. The longer the arm, the larger moment, thus producing higher sensitivity. A generic torsional pendulum thrust stand design can be seen if Figure (1.1).

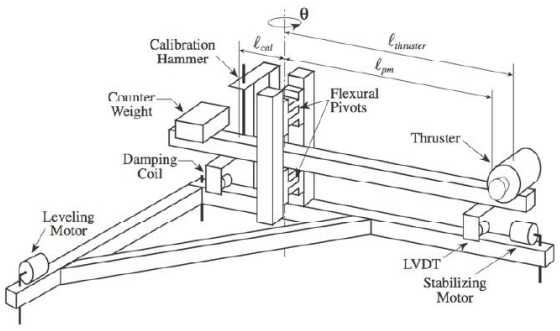

Figure 1.1: Example Concept of Torsional Pendulum Thrust Stand [**13**]

Hanging Pendulum Thrust Stand

Similar to the torsional pendulum, the hanging pendulum thrust stand has a moment arm system, however in this case, the arm is vertical. The vertical arm is connected to a base with a pivot while the thruster is placed at the far end of the arm. Paralleling the torsional design, displacement sensing, dampening, and calibration systems are also used. This stand design benefits from having better heat resilience than torsional stands due to the arms often being longer. Yet again, a longer pendulum arm will increase sensitivity. Unlike the torsional stand, due to the arm being in the vertical configuration, gravity is no longer negligible and must be added to calculations. Figure (1.2) depicts a basic conceptual image of a hanging thrust stand.

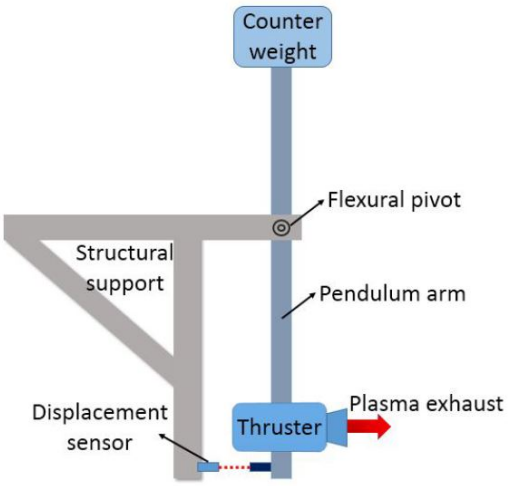

Figure 1.2: Example Concept of Hanging Pendulum Thrust Stand [**4**]

Inverted Pendulum

Inverted pendulums are useful when needed for compact areas and high sensitivity. An inverted pendulum has a vertical arm similar to the hanging stand, however the thruster is mounted at the highest point of the arm with a pivot located at the lowest point of the arm. This is to have the center of mass above the pivot. For this thrust stand, the dampening load spring is added to counteract larger angular deflections of the stand. Although inverted stands take up less space, they are poor thermal dissipators due to the limited amount of material. Figure (1.3) shows a schematic for basic conceptual understanding of inverted pendulums.

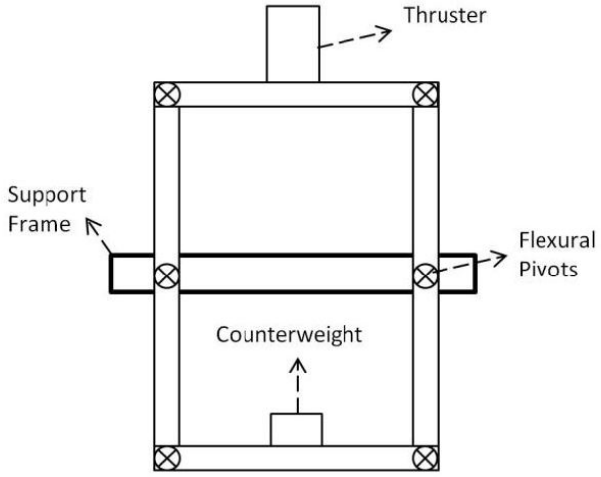

Figure 1.3: Example Concept of Inverted Pendulum Thrust Stand [**6**]

Chapter 2

Project Introduction

2.1 Problem

Due to technological advancements and affordability, EP has been gaining a lot of interest. There are now three organizations that conduct research with electric propulsion devices that WMU's College of Engineering and Applied Sciences (CEAS) are affiliated with. The Aerospace Laboratory for Plasma Experiments (ALPE) directed by Dr. Kristina Lemmer researches plasma devices for space propulsion, plasma physics, plasma diagnostic techniques, and modeling of plasmas. The Western Aerospace Launch Initiative (WALI) is a student run organization at CEAS that develops cube satellites to be launched to space. WALI's current design iteration called Performance of Electrospray Propulsion on Ground and in Space (PEP-GS) CubeSat plans to use an EP thruster and compare the performance of on-ground vacuum chamber testing to on-orbit performance. Additionally, ALPE is working with the propulsion system of another cube satellite team called Space Weather Atmospheric Re-configurable Multiscale Experiment (SWARM-EX) CubeSat. SWARM-EX is planning on using a low thrust thruster on their satellite.

These organizations currently don't have a way to directly measure thrust from their thrusters. The thrust data is crucial to confirming validity of analytical thrust models, indirect thrust measurement, and for thruster performance and efficiency testing; additionally, the data can be mission critical for the CubeSat teams. Thrust stands are custom built for different thrusters and not commercially available. Furthermore, since multiple organizations are in need of direct thrust measurements, different size thrusters will be used. A modular and re-configurable solution is necessary to accommodate the different thrusters that might be used. In addition, the proposed design ideally should be inexpensive and easily replicable so other growing electric propulsion teams could have the option to use the design.

2.2 Objective

The flexure, optical sensing, damping and leveling systems for a thrust stand originally designed by Hannah Watts in her WMU Honors Thesis: Design of A Thrust Stand for Electric Propulsion [**18**] will be completed. These systems will be redesigned, optimized, and finally constructed to be integrated into the thrust stand structure. The final product will be a fully functioning thrust stand that has been

verified with extensive testing and usable by each of the aforementioned organizations. Each subsystem will be designed for compatibility between different EP thrusters. Additionally, substantial documentation will provided to allow for reconfiguration, ease of use, and easy replication.

2.3 Scope and Limitations

The project has multiple success criteria that arise from the different subsystems and primary system. The leveling system of the thrust stand shall be able to level the system to have the pendulum arm horizontal with the gravity vector. The flexure system shall have a low friction pivot with a dampening ratio that allows for the use of multiple different thrusters. The optical sensing system shall measure the displacement of the arm with high levels of sensitivity and accuracy. The thrust stand shall measure a displacement produced by a low thrust propulsion device, and convert the displacement to a true thrust value all while being re-configurable for the use of multiple propulsion devices.

Chapter 3

Design

3.1 Specifications and Requirements

Specifications will drive the design criteria and provide guidelines for construction and implementation of the various subsystems.

- Measurement Accuracy

  With the intention to equip several different thrusters to the EP thrust stand a broad measurement range is required. The proposed thrust measurement range: $10\mu N$ to $1mN$ is adequate for the various thrusters intended to be analyzed. Ideally the measurement accuracy for the thrust stand is $10\mu N$.

- Compatibility

  The thrust stand subsystems will be designed to accommodate several different EP thrusters. This decision will have significant impact on the design of the subsystems. EP thrusters can have significantly different weight and thrust outputs. The flexure pivots and leveling systems will be required to support and adjust (level) the varied weight load. Additionally, the response of the damping system is tied to the moment of inertia of the rotating arm which will change with weight. This system will have to be variable to allow for adjustments each time a new thruster is equipped.

- Timeline

  The current deadline for construction and system integration of the EP thrust stand is April 2022. The SWARM-EX CubeSat team will have a EP thruster prepared by that time and the goal is to support their thruster testing with the proposed thrust stand equipped with the designed subsystems. In the case of the damping subsystem, this subsystem will have to be tuned to accommodate the SWARM-EX thruster's weight and thrust outputs to allow for accurate measurement.

- Documentation

  Currently EP thrust stands are custom built for the specific thruster they test. One goal of this project is to provide documentation that allows for the recreation of the designed thrust stand components. Complete with procedures for operation and tuning for other growing EP teams.

3.2 Constraints

While the requirements of the individual subsystems may vary, each must adhere to a basic set of constraints due to the nature of the project:

- Size

  The ALPE large vacuum chamber is the proposed host for the EP thrust stand. This vacuum chamber is a 1.5-m long by 1-m diameter cylinder. Inside the chamber is cubic structural framing made of 80/20 aluminum. This framing will be the attachment pad for the thrust stand. The usable space within the framing is limited to 31 x 40 x 24.5 inches (L x W x H).

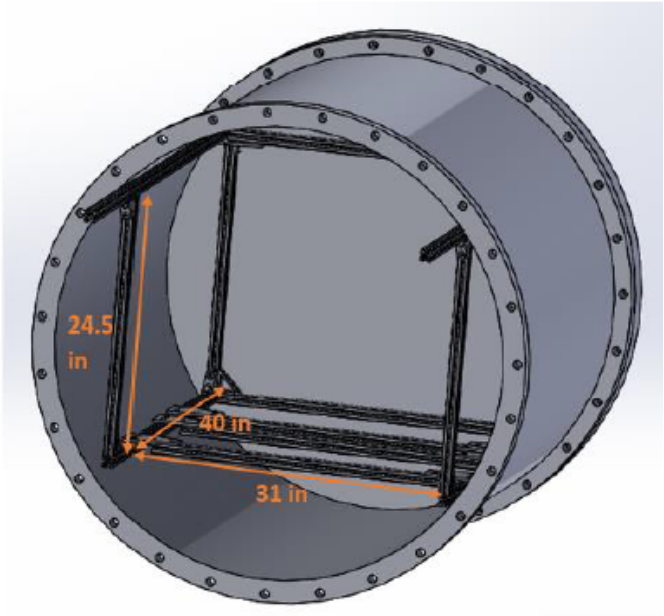

Figure 3.1: ALPE Chamber 80/20 Structure

- Vacuum Environment

  All materials that the subsystems are constructed with must be safe for use in a vacuum chamber. Certain materials when exposed to low pressure environments will either outgas absorbed gasses or evaporate gasses from the material itself. Materials to avoid include Cadmium, Zinc, Lead and many plastics for example. The gasses released can be toxic or cause contamination. To prevent any hazards the subsystems need to be constructed of vacuum safe materials. 304 stainless, aluminium, and Macor are a few of the materials that can be used. The expected level of pressurization for high vacuum within the chamber ranges from $1 * e^{-3}$ to $1 * e^{-7}$ Torr.

- Cost

  This project aims to be as economical as possible such that any results can be replicated by other universities and research institutions. Although the budget for this specific project was loose, whenever practical, lower cost options were often explored and investigated and cost was a factor in all decisions. From previous design iterations, certain components and material had already

been purchased. To reduce costs, the purchased materials were used to drive decision choices and used on the current design.

3.3 Subsystem Design

3.3.1 Leveling System

The leveling system's purpose is to make sure that the pendulum arm is perpendicular to the gravity vector. The can be accomplished by balancing the stand on three points, one of which is just an anchor point. By adjusting the other points up or down, the system can be independently leveled on both the x and y axis. There are a few ways to adjust the points, either via motorized adjustment or manual adjustment. The main criteria when determining what is best for the system are: cost, travel distance, max load capacity and size. Motorized actuators in the form of an inertia actuator or servo motor have the key advantage that they would be able to be adjusted while in use even when the thrust stand is in the vacuum chamber. They do, however, have a massive downside which is a very large cost. Manual adjustment such as with a micrometer has a much lower cost but will have to be adjusted before the thrust stand has entered the chamber. Table (3.2) compares different commercial actuators in a decision matrix to determine the best method for this design. A simple 1-4 scale where a score of 1 denotes a poor fit for a criteria while a score of 4 is a great fit with the criteria. The designs with the highest score were selected for consideration. Table (3.1) shows the scale for the matrices.

Scale	1	Poor
	2	Adequate
	3	Good
	4	Great

Table 3.1: Decision Matrix Scale

	PIAK10VF	Z806-V	8301-V	N-111.201	SM-13	SM-25	MH-2500
Cost	1	1	1	1	4	4	3
Travel Distance	3	4	3	3	3	4	3
Max Load Capacity	2	2	3	4	2	4	2
Size	4	4	4	3	4	4	2
Total	10	11	11	11	13	24	10

Table 3.2: Leveling System Decision Matrix

A full table with the full characteristics of each can be found in appendix (A2).

With the SM-25 Micrometer scoring the highest, it was decided to use this for the leveling system. The main benefits of the SM-25 was the high load capacity with low cost and simplistic design. Figure (3.2) shows the SM-25 micrometer.

Figure 3.2: SM-25 Micrometer

A mounting solution for the micrometers was designed to securely hold the micrometers to the thrust stand. Simple square brackets were designed and constructed to use the included threading from the manufactured unit. Figure (3.3) is the CAD model of the intended bracket, the machine drawing for the bracket can be found in Appendix A, and lastly Figure (3.4) is the final machined part.

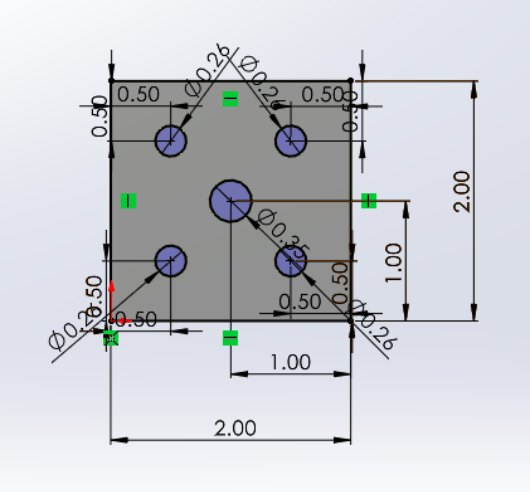

Figure 3.3: Micrometer Bracket CAD

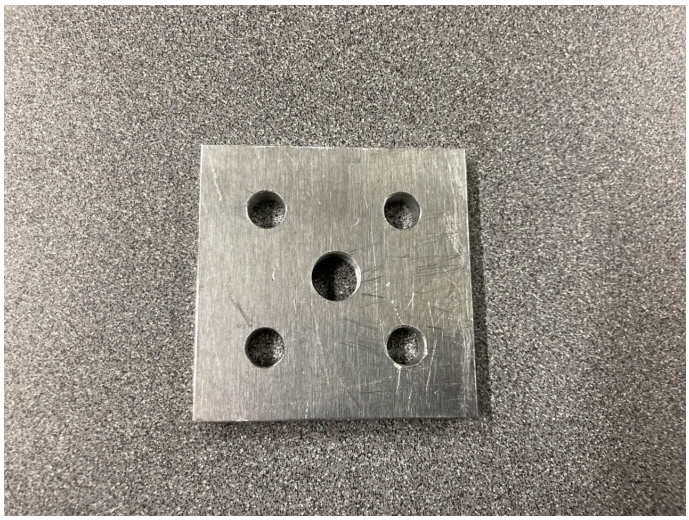

Figure 3.4: Machined Micrometer Bracket

Additionally, V-channels were designed to attach to the thrust stand base in order to guide the micrometer feet into a secure position to lock the thrust stand into position. The CAD for the V-channels is provided in Figure (3.5), with machine drawing in Appendix A, and the machined part in Figure (3.6).

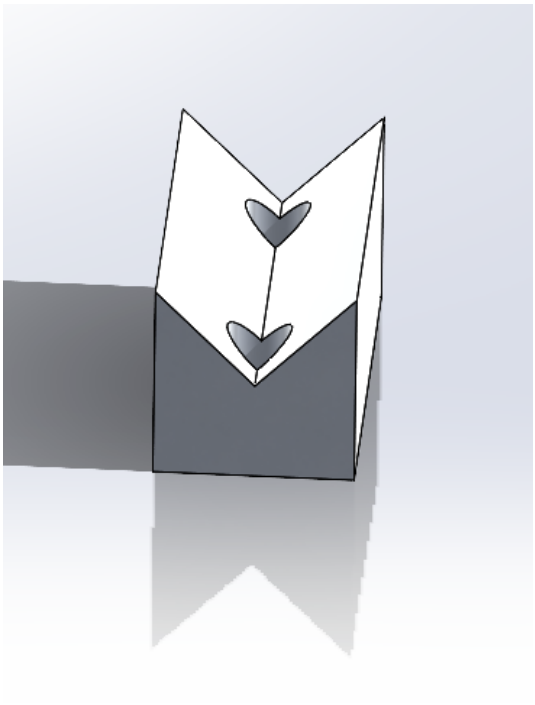

Figure 3.5: V-Channel CAD

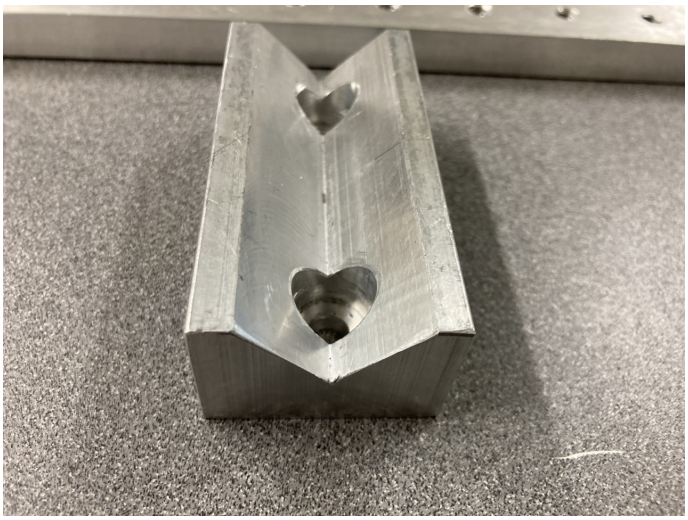

Figure 3.6: Machined V-Channel

These elements of the leveling system are located at the far ends of the thrust stand base arms. CAD for the assembled leveling system can be seen in Figure (3.7) with the completed system in figure (3.8).

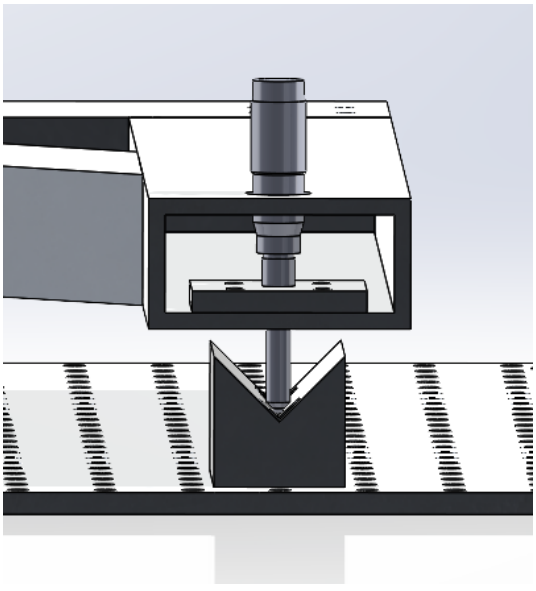

Figure 3.7: Leveling System CAD

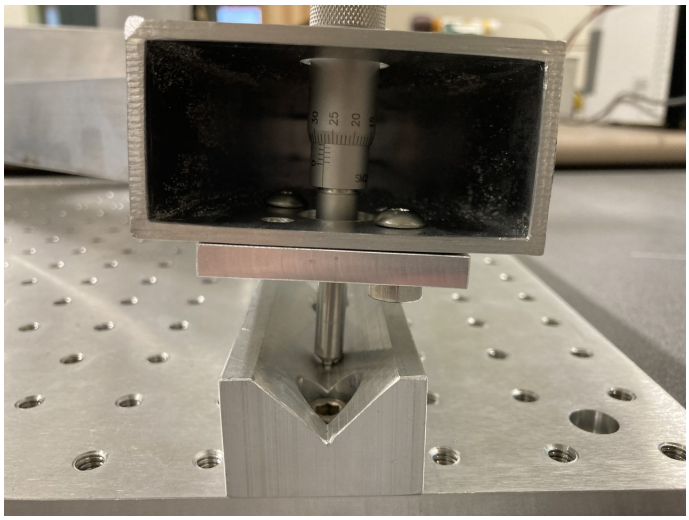

Figure 3.8: Complete Leveling System

Additionally, an inclinometer sensor, which was purchased in the last iteration of the thrust stand design, will be used to ensure the system is level within the vacuum chamber. The sensor is the Analog Devices ADIS16209 chip which is a high speed SPI inclinometer/accelerometer that is mounted onto a breakout PCB This breakout board had many other pinouts that aren't used for basic communication and use. The breakout board is separated into two sets of 12 pinouts via J1 and J2. Wires can be connected to the pinouts with normal soldering techniques or with a 12-pin dual row 2mm connector. The ADIS16209 can use a voltage ranging from 3.0 V to 3.6 V. This includes the SPI communication lines. This must be double checked if a different microcontroller is used, even if a microcontroller has a 3V output line, the SPI could be 5 V.[**1**]

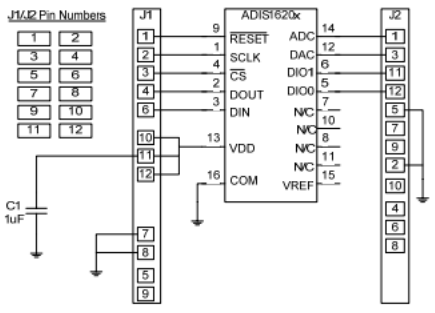

Figure 3.9: ADIS16209 Pinouts (Courtesy of Analog Devices)

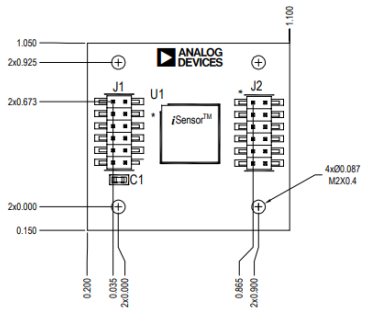

Figure 3.10: ADIS16209 Mechanical Specifications (Courtesy of Analog Devices)

It should be noted that there is a place for a capacitor at C1, this is for power supply smoothing if the supplied power isn't very good. As mentioned previously, the ADIS16209 uses SPI serial protocol for communication. There are 4 main SPI pins that need to be connected to a controller or master for proper communication.

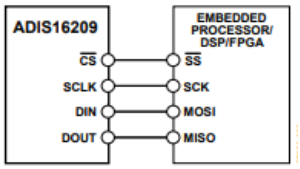

Figure 3.11: Basic ADIS16209 Wiring Diagram (Courtesy of Analog Devices)

Mnemonic	Function
SS	Slave Select
SCLK	Serial Clock
MOSI	Master Output Slave Input
MISO	Master Input Slave Output

Table 3.3: ADIS16209 Mnemonics

The MOSI and MISO line are where the communication between the devices will take place, while the SCLK is the running clock that allows for the communication to perform on the same proper time. The SS or slave select pin selects the slave that will be receiving the command. When the line is written as "LOW" the slave listens to the Master, but when the line is written "HIGH" the slave no longer listens to the slave. This will be important later when fully integrating the system into the thrust stand since both devices should be running. The SPI configuration settings are provided in table (3.4). These should be coded within the microprocessor for proper master control.

Processor Setting	Description
SCLK ≤ 1 MHz	Maximum serial clock rate is less than or equal to 1 MHz
SPI MODE 3	CPOL = 1 (Polarity), CPHA = 1 (Phase)
MSB First Mode	Bit sequence
16-Bit Mode	Shift Register and data length

Table 3.4: SPI Configuration Settings

The SPI protocol for the chip requires two 16-bit cycles. One requests the contents of a register and the other receives the contents of the register. For the read request, there are three parts: A read bit (R/W = 0), address of the register [A6:A0], and eight don't care bits [DC7:DC0]. A list of the register addresses is provided in Figure (3.12).

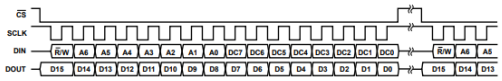

Figure 3.12: SPI Bit Sequence (Courtesy of Analog Devices)

A full list of the ADIS 16209 commands can be seen in figure (3.13).

Name	R/W	Flash Backup	Address	Size (Bytes)	Function	Reference
ENDURANCE	R	Yes	0x00	2	Diagnostics, flash write counter (16-bit binary)	
SUPPLY_OUT	R	No	0x02	2	Output, power supply	Table 20
XACCL_OUT	R	No	0x04	2	Output, x-axis acceleration	Table 10
YACCL_OUT	R	No	0x06	2	Output, y-axis acceleration	Table 11
AUX_ADC	R	No	0x08	2	Output, auxiliary ADC	Table 22
TEMP_OUT	R	No	0x0A	2	Output, temperature	Table 18
XINCL_OUT	R	No	0x0C	2	Output, ±90° x-axis inclination	Table 13
YINCL_OUT	R	No	0x0E	2	Output, ±90° y-axis inclination	Table 14
ROT_OUT	R	No	0x10	2	Output, ±180° vertical rotational position	Table 16
XACCL_NULL	R/W	Yes	0x12	2	Calibration, x-axis acceleration offset null	Table 32
YACCL_NULL	R/W	Yes	0x14	2	Calibration, y-axis acceleration offset null	Table 32
XINCL_NULL	R/W	Yes	0x16	2	Calibration, x-axis inclination offset null	Table 33
YINCL_NULL	R/W	Yes	0x18	2	Calibration, y-axis inclination offset null	Table 33
ROT_NULL	R/W	Yes	0x1A	2	Calibration, vertical rotation offset null	Table 33
			0x1C to 0x1F	4	Reserved, do not write to these locations	
ALM_MAG1	R/W	Yes	0x20	2	Alarm 1, amplitude threshold	Table 34
ALM_MAG2	R/W	Yes	0x22	2	Alarm 2, amplitude threshold	Table 34
ALM_SMPL1	R/W	Yes	0x24	2	Alarm 1, sample period	Table 35
ALM_SMPL2	R/W	Yes	0x26	2	Alarm 2, sample period	Table 35
ALM_CTRL	R/W	Yes	0x28	2	Alarm, source control register	Table 36
		No	0x2A to 0x2F	6	Reserved	
AUX_DAC	R/W	No	0x30	2	Auxiliary DAC data	Table 30
GPIO_CTRL	R/W	No	0x32	2	Operation, digital I/O configuration and data	Table 29
MSC_CTRL	R/W	No	0x34	2	Operation, data-ready and self-test control	Table 28
SMPL_PRD	R/W	Yes	0x36	2	Operation, sample rate configuration	Table 24
AVG_CNT	R/W	Yes	0x38	2	Operation, filter configuration	Table 26
SLP_CNT	W	Yes	0x3A	2	Operation, sleep mode control	Table 25
STATUS	R	No	0x3C	2	Diagnostics, system status register	Table 37
COMMAND	W	No	0x3E	2	Operation, system command register	Table 31
		No	0x40 to 0x49	10	Reserved	
PROD_ID	R	Yes	0x4A	2	Product identification = 0x3F51	N/A

Figure 3.13: SPI ADIS16209 Commands (Courtesy of Analog Devices)

3.3.2 Optical Sensing System

There are two main common practices for displacement measurement in thrust stands. The first one uses a Fiber Optic Displacement Sensor, such as the one utilized in this project. The other method uses a Linear Voltage Differential Transformer (LVDT). In the design of a thrust stand, the implementation of either type of displacement measurement is a matter of preference. However, the advantages and disadvantages of an LVDT are explained below.

- Linear Voltage Displacement Transformer (LVDT)

  An LVDT is composed of a core and two outer windings. The core will move linearly inside the windings when contact is made. As the core moves out of the null position, an electric flux is generated and the voltage difference between the two windings is altered. In principal, the voltage difference is proportional to the displacement of the core. This voltage change would me measured using some sort of Data Acquisition (DAQ) and Instrumentation method, such as LabVIEW, and displacement will be calculated based on the specifications of the specific LVDT being used. The advantage of this is that LVDTs are very ubiquitous. The big disadvantage is that and LVDT requires

contact with the torsional arm to measure displacement. For that reason, an Optical Sensor was chosen instead.

The Fiberoptic Digital Displacement Sensor used in this torsional thrust stand is the mDMS-D64 which is produced by Philtec Inc. in Annapolis, Maryland. The mDMS-D64 has an operating range of 6mm (240m INCH). To interface the mDMS-D64 with the WMU ALPE vacuum chamber, A Bv-133 swagelock-fitted feedthrough is used. The Bv-133 is also produced by Philtec Inc. and allows the optical sensor to interface with vacuum chambers under operating parameters of 10 E-7 Torr. The figures below show illustrations of each product being implemented.

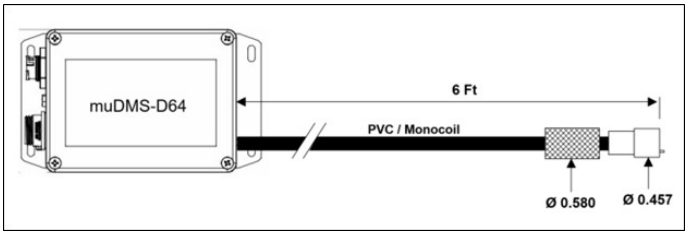

Figure 3.14: muDMD-D64 (Courtesy of Philtec)

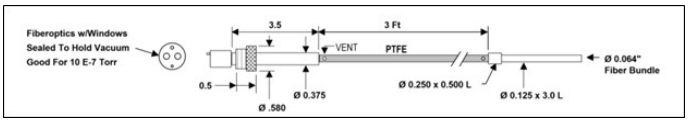

Figure 3.15: Bv-133 10E-7 Torr Feedthrough (Courtesy of Philtec)

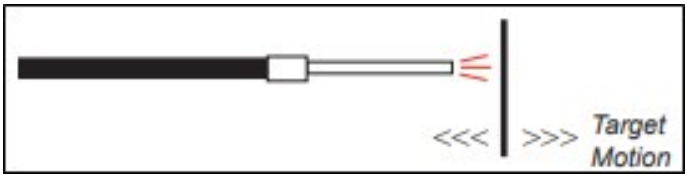

Figure 3.16: Optical Sensor and Target Motion Configuration (Courtesy of Philtec)

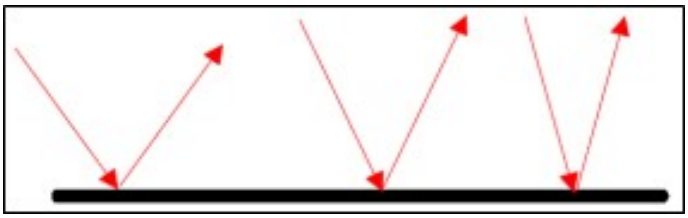

Figure 3.17: Mirror Reflectance of Signal Emitted from Fiberoptic Sensor (Courtesy of Philtec)

Figure 3.18: Optical Sensor Displacement Data Output in Philtec DMS Control Software (Courtesy of Philtec)

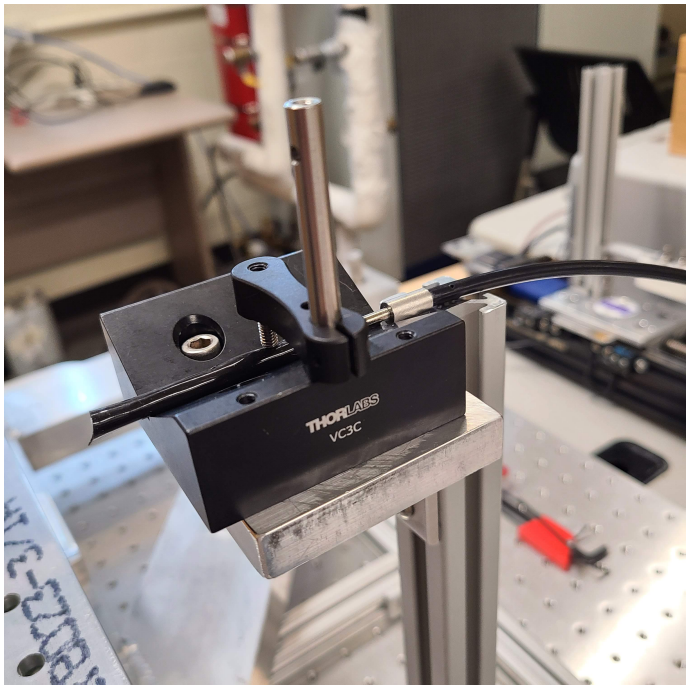

Figure 3.19: Optical Sensor Mounted to Thrust Stand

The Fiberoptic Displacement Sensor works by using fiberoptic wiring to emit a signal towards a surface. These waves are the reflected back towards the sensor as input. This input data is fed through the wiring and back into the computer of which it is interpreted as a voltage difference. This voltage difference is sent as a digital signal and interpreted by the Philtec DMS Control Software. The software then reports back many metrics including: Reflectance, Distance (Displacement), Peak-to-Peak Amplitude, and others. Additionally, configurations can be set for the type of reflective surface being used. Mirrors and other highly reflective materials

produce the best results. The configuration of target reflectance shifts the output voltage higher or lower to produce a more accurate reading for the software to interpret. The figures above demonstrate how the sensor works and examples of how the output data is displayed. A decision matrix was created to determine the best displacement sensor for they system using the same scale as Table (3.1).

	Displacement Sensors			
	muDMS-47	muDMS-D63	muDMS-64	muDMS-100
Cost	2	3	3	2
Vacuum Rating	4	4	4	4
Operating Range	3	2	4	4
Total	9	9	11	10

	Vacuum Feed-Thru Products		
	Bv1	Bv133	Bv2
Cost	4	3	1
Vacuum Rating	4	4	2
Compatability	1	3	3
Total	9	10	6

Table 3.5: FiberOptic Displacement Sensor Decision Matrix

3.3.3 Pivot System

In torsional thrust stand design and construction, it is traditional to utilize flexure pivots to allow the rotation of the torsional arm about an axis with known spring constants. Flexure Pivots are proven to be robust, accurate, and reliable for this exact application. Jewel Bearings were briefly considered but were quickly deemed not not adequate for this application.

- Felxure Pivot

  Flexure Pivots are commonly used in space and other applications where mechanical components must operate under vacuum conditions. This design utilizes two (2) I-30 Flexure Pivots which are arranged co-axially in the flexure arm of the Thrust Stand. These pivots have a known torsional spring rate (TSR) of 3.261 in*pound/degree.

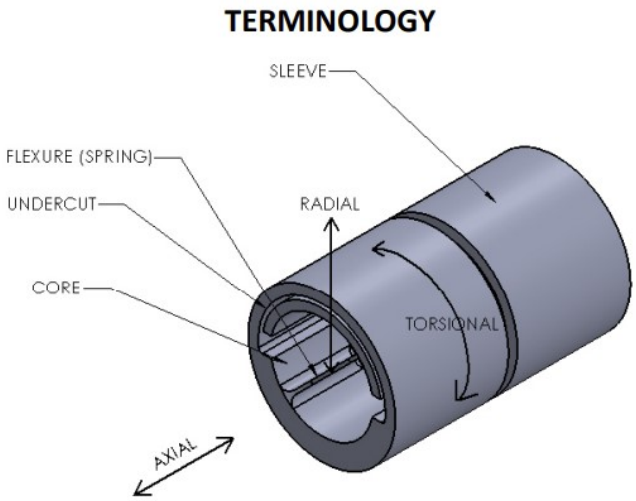

Figure 3.20: General Model of a Flexure Pivot (Courtesy of C-Flex)

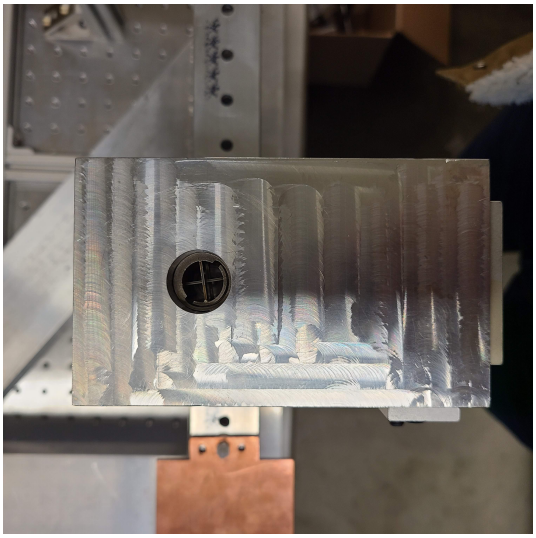

Figure 3.21: Flexure Assembly (Top Down)

The known TSR is vital to the displacement, and consequently the thrust due to the mathematical relation below:

$TSR = \tau \times \theta$ where τ is torque (in. $\times$ pounds) $\tau = F \times L$, where F is thrust (pounds) and L is the torsional arm length (inches). $\Theta = \delta \times L$, where δ is measured linear displacement.

This is the fundamental mathematics for which thrust will be calculated. All data can be calculated and converted in between English and SI units.

- Jewel Bearing

  Jewel bearings are a type of mechanical gear bearing mostly known for use inside luxury watches. These bearings are known for being incredibly precise. Jewel bearing were ultimately decided against due to their fragility and complexity. These disadvantages increase the odds of failure of the bearing as

opposed to the much simpler flexure pivot. Additional, jewel bearings are expensive and may require lubrication that renders them inadequate for vacuum applications.

A decision matrix, using the scale in Table (3.1), was created to select the best flexure system.

	G-30	H-30	I-30	J-30
Cost	4	3	3	2
Diameter Fit	2	3	4	1
Max. Deflection	2	3	3	1
Spring Constant	2	3	3	1
Max Radial Loading	1	2	3	4
Earliest Availability	1	4	4	1
Total	12	18	20	10

Table 3.6: Flexure Pivot Decision Matrix

3.3.4 Damping System

Controlling vibration while minimizing drift were the primary goals for this system. Due to the expected range of thrust force values ($140\mu N$ to $55mN$) the only damping methods explored involved Electromagnetic (EM) Dampers. EM Damping systems provide contact-less force input that can be used to damp the thrust impulse. This completely removes friction from the system. Additionally, these techniques can be expanded into a calibration system, but is currently outside of the scope of this project. The following are two electromagnetic damping options explored for this project are:

- Permanent Magnet - Solenoid Interaction

  The basis for this technique consists of either a single or set of magnets arranged in a fashion that produce a magnetic field. A solenoid is then placed a certain distance or directly around the magnet's field. As the thrust arm would rotate laterally, the damper would be configured to either push, or pull against the thrust arm. By adjusting the current flowing through the solenoid one can manipulate the field generated by the solenoid and tune the strength of the damping force. The magnet or the solenoid can be fixed to the thrust stand's rotating arm, while the other is rigidly mounted to the base. [**2**]

  This design has the advantage of being variable and as described is considered open-loop control. By tuning the current the effect of the damping system can be manipulated. With further development past the scope of this project, this design could be converted to closed-loop control based around current authority.

  This method also had some disadvantages, modeling magnetic field interactions between a solenoid and a permanent magnet is not trivial. This is due to the fact that when the thrust arm begins to rotate the magnet is no longer centered within the solenoid and will turn. Consequently, the magnetic field interactions are not longer perpendicular or equal around the magnet.

This can be accounted for but adds significant complexity. Size concerns can be an issue because this style of damper is mounted on one side of the thrust arm in the plane of rotation. Due to the expected small angles of a torsional thrust stand deflection the lateral width of the stand is often smaller than the length. The increased width of the stand can be a concern for smaller vacuum chambers.

- Eddy Currents

  The basis for this control technique relies on the generation of Eddy Currents within a conductive plate. The layout for this damping system includes a conductive plate moving through a magnetic field. The relative motion between the magnetic field and a perpendicular conductive plate will generate electric currents (Eddy Currents) within the conductive plate. This is an example of Faraday's Law of Induction. According to Lenz's Law, an eddy current creates a magnetic field that opposes the magnetic field that created it. As a result, the relative motion and subsequently created magnetic field will generate a damping force between the magnetic field source and the conductive plate's newly generated magnetic field. The two primary methods of generating a magnetic field are using permanent magnet or an electromagnet. [**14**][**10**]

  Electromagnets are a convenient for this purpose due to their ability to adjust the strength of their magnetic field by changing the applied current, which will change the damping strength. This can be done on the fly from outside the vacuum chamber or incorporated into a feedback system using a controller to constantly alter the field strength for optimum damping. Another level of adjustment for the damping force is done by altering the distance between the conductive plate and the field source. This method applies to both electromagnetic and permanent magnets.

  To adjust the damping force for a permanent magnet the distance between the conductive plate and the magnetic must be adjusted. If the permanent magnet has a rigid mount this can only be done before the thrust stand is placed in the chamber. This is inconvenient if the damping has to be adjusted during testing. Additionally, there is no way to turn off the damping from this configuration. Mounting the permanent magnet on a vertical linear stage provides the ability to adjust the magnetic field strength from outside the vacuum chamber.

  The force generated by the eddy current damper is heavily influenced by the geometry of the conductive plate. The damping force is proportional the velocity of the thrust stand arm. As shown below in Equation 3.1.

$$F = -\sigma\delta SVB^2 \text{ [10]} \tag{3.1}$$

  F = force opposing relative motion, σ = conductive coefficient, δ = thickness of the conductive metal, S = surface area of the conductive metal, V = relative velocity, B = strength of the magnetic field perpendicular to plate

The velocity of the torsional thrust arm is expected to be very small due to the fact that the torsional arm will only displace $\theta < 1$. As a result of this, the

majority of the velocity of the torsional arm will come from vibration and other noise. Machinery vibration can range from good levels: $< 5.0mm/s$ to rough levels: $> 10mm/s$. Predicted velocity level are expected to be at or less than $< 5.0mm/s$. [**19**]

An Eddy Current Damper was developed to damp the torsional thrust arm. This design should provide good adjustments for compatibility with different thrusters and have a relatively small footprint when attached to the thrust stand. A damping ratio of $0.4 < \zeta < 0.8$ will be a design goal. This comes from Recommended Practice for Thrust Measurement's in Electric Propulsion Testing to provide a good response time to a step input.[**13**]

Shown below is a decision matrix between selecting a magnet/coil versus eddy current arrangement.

	Damping Configuration	
	Magnet/Coil	Eddy Current
Cost	2	2
Ease of setup	2	3
Analytical Model Difficulty	3	2
Performance	3	3
Size	2	3
Magnetic Field Interference	2	3
Documentation	3	2
Total	17	18

Table 3.7: Damping Decision Matrix

3.3.5 Electromagnet

Initially, an electromagnet was select as the source of the magnetic field for the damper. Two separate adjustment axes: vertical height and applied current, would provide a large range of damping force for multiple different thrusters. The vertical height would be set prior to sealing the vacuum chamber and the current flowing through the electromagnet would be used to tune the damping during testing. The proposed eddy current damper will consist of an electromagnet and a copper plate. The copper plate will be attached to the underside of the torsional arm and electromagnet will be attached to an "L" bracket with multiple vertical mounting locations for different vertical height distance settings.

This damping control system is considered open loop. Adjustments to damping will be made before/after the test run is complete when the chamber is opened. Using the proposed design sets up the potential of future work to incorporate a closed loop control system to the damper. Data from the optical sensor could be used to vary the strength of the electromagnet on the fly using a PID and real time velocity input. This however is currently outside the scope of the current project. An early exploded CAD model is shown below.

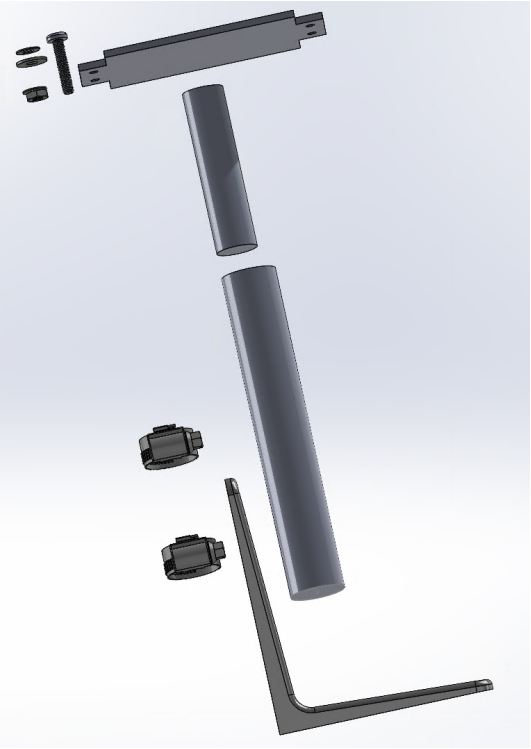

Figure 3.22: Early CAD of Electromagnet Damper (windings not shown)

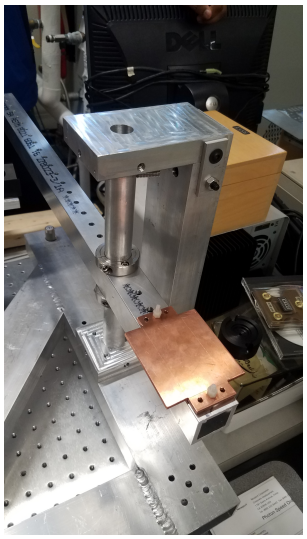

Figure 3.23: Copper Plate attached to Torsional Arm

Multiple mount options were considered for attaching the copper plate to the torsional arm. One important feature of the plate mount is to electrically isolate the copper plate from the aluminum torsional arm. Non-conductive hardware in the form of PTFE screws, PTFE nuts, and ceramic washers were the best option cost wise. The copper plate will be bolted directly to either side of the torsional arm depending on configuration. The copper plate itself was purchased second hand from an online scrap retailer and cut to size. This dramatically reduced the cost in acquiring a new relatively thick, piece of copper. A CAD drawing of the copper plate can be found under Appendix A.

Dimension wise, the copper plate's area was intended to be 3 times the surface area of the electromagnet's face to completely encapsulate the generated magnetic field. This ended up being roughly a 3 in x 3 in square piece of copper plate. "Wings" were added to the each side of the square plate to provide mounting locations for the screws. This method would leave the center of the square plate uninterrupted for the entire magnetic field to interact with.

A test electromagnet was created as a proof of concept from a 3D printed housing, iron core, and spare wire. The final intended housing would be made of a machinable ceramic called Macor. To keep costs low Delrin, a vacuum compatible acetal plastic was selected in lieu of the Macor. Triple insulated PTFE wire was gifted at no cost from Phoenix Wire. This wire has favorable out-gassing rates and would create the final electromagnet. Testing of the ABS plastic and delrin electromagnets highlighted the short comings of this design. Shown below are the two electromagnetic being tested using a Guass meter.

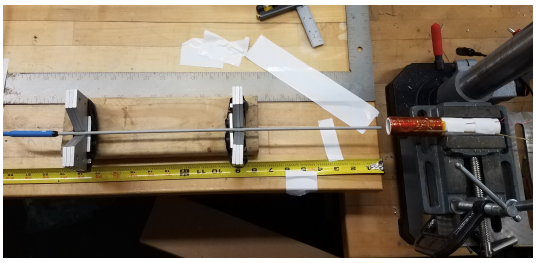

Figure 3.24: Wood Dowl Electromagnet

Figure 3.25: Delrin Electromagnet

Coil heating was expected to be a minor inconvenience, this was a gross miscalculation. A thermocouple was wrapped within the windings to measure the temperature. This would be used to notify the operator to turn off the electromagnet before it would damage itself. An early solution to this problem included using a standard duty cycle: "Operate for x minutes then rest for y". This would not be compatible with long duration thruster testing. The coil regularly reached unsafe levels (in excess of 150 C) and was struggling to cool down in a reasonable time frame while in atmosphere. This problem would be compounded when operated in a vacuum chamber. Additionally, the magnetic field generated by the electromagnet was smaller than expected, increased amperage to compensate for this discrepancy only made the heating problem worse.

To remedy the heating issue a water cooling loop would need to be created. Pass through ports on the bulkhead of the vacuum chamber would allow for coolant water to flow into and out of a hollow copper coil wrapped around the electromagnet. These copper coils are commonly used to cool RC electric boat motors, are conveniently were the correct size to fit outside the windings. Outside the chamber a pump, radiator, and fan would remove heat from the system.

This potential solution added unnecessary cost and complexity to the design. Not to mention water leaks within the chamber would be disastrous and significantly increase the number of failure points. Also, conducting the heat from the coils to the copper cooling jacket would be difficult without an expensive vacuum rated thermal interface pad. The electromagnet idea was abandoned in favor of a permanent magnet solution. This pivot to a permanent magnet meant the only control available involved altering the distance between the permanent magnet and the copper plate.

3.3.6 Permanent Magnet

Although much of the work involved with the development of the electromagnet would not be used in the final damping solution, some parts could be repurposed. On the torsional arm side of the damper nothing would change, the existing conductive plate and mounting solution would be sufficient for the permanent magnet. The "L" bracket mounting system originally designed to support the much larger electromagnet would still work to support a permanent magnet in a wide range of vertical heights. This would be a rigidly mounted system that could only be adjusted when the chamber was open, but would work on an tight budget. To regain adjustability, a linear stage system would be used to raise and lower the permanent magnet allowing damping control from outside the sealed chamber.

3.3.7 Damping Analysis

The starting point to determine the strength of the permanent magnet required was to analyze the equation of motion for the system using standard second order underdamped dynamic modeling techniques. Shown below is a simplified free body diagram of the torsional arm.

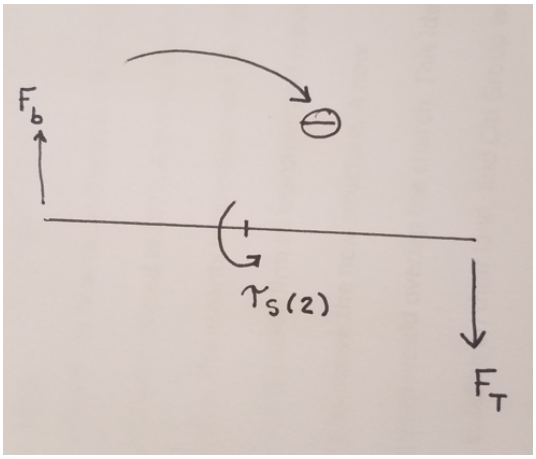

Figure 3.26: Torsional Arm FBD

F_T = force of thrust, F_b = force of damper, τ_s = spring torque, θ = direction of rotation The length of the distance between the thruster and the point of rotation is: l_t, and the length of distance between the thruster and the point of rotation is: l_b.

$$\begin{aligned} \tau_T &= l_t F_T \\ \tau_b &= l_b F_b = b\dot{\theta} \\ \tau_s &= k\theta \\ I\ddot{\theta} &= \tau_T - 2\tau_s - \tau_b \end{aligned} \tag{3.2}$$

θ = angular position, $\dot{\theta}$ = angular velocity, $\ddot{\theta}$ = angular acceleration, I = moment of inertia, k = spring constant, b = damping constant

The Laplace transformation was used with no initial conditions.

$$\begin{aligned} \mathcal{L}[I\ddot{\theta} = \tau_T - 2\tau_s - \tau_b] \\ I\theta(s)s^2 + s\theta(0) - \theta(0) + bs\theta(s) - \theta(0) + 2k\theta(s) = \tau_T(s) \\ I\theta(s)s^2 + bs\theta(s) + 2k\theta(s) = \tau_T(s) \\ \theta(s)(Is^2 + bs + 2k) = \tau_T(s) \\ \frac{\theta(s)}{\tau_T(s)} = \frac{\frac{1}{I}}{s^2 + \frac{b}{I}s + \frac{2k}{I}} \\ a_0 = \frac{2k}{I} \\ a_1 = \frac{b}{I} \\ a_2 = 1 \end{aligned} \tag{3.3}$$

a_0, a_1, a_2 = coefficients

From this information and using Equation 3.1 we can predict the damping constant (b) of a system using the velocity and the resulting force. $F_b = b(V_2 - V_1)$. The graph below displays the ideal dissipative energy between the interaction between a copper plate with the same dimensions as above (3.175mm thick, .005806 m^2 area) within a 0.5 Tesla magnetic field. The velocities used for this approximation are from low to severe vibration. [**19**]

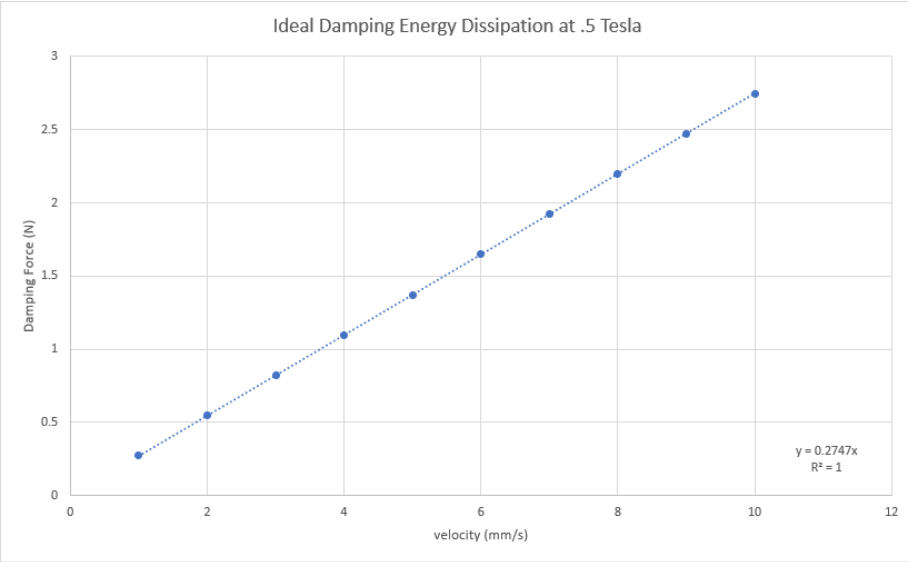

Figure 3.27: Ideal Damping Energy Dissipation

The slope of the line is equal to the ideal damping constant, this will vary with the strength of the magnetic field. For a 0.5 Tesla permanent magnet the damping constant is approximately: $0.2747 Ns/m$. This can be expanded on by varying the strength of the magnetic field, the results are show below.

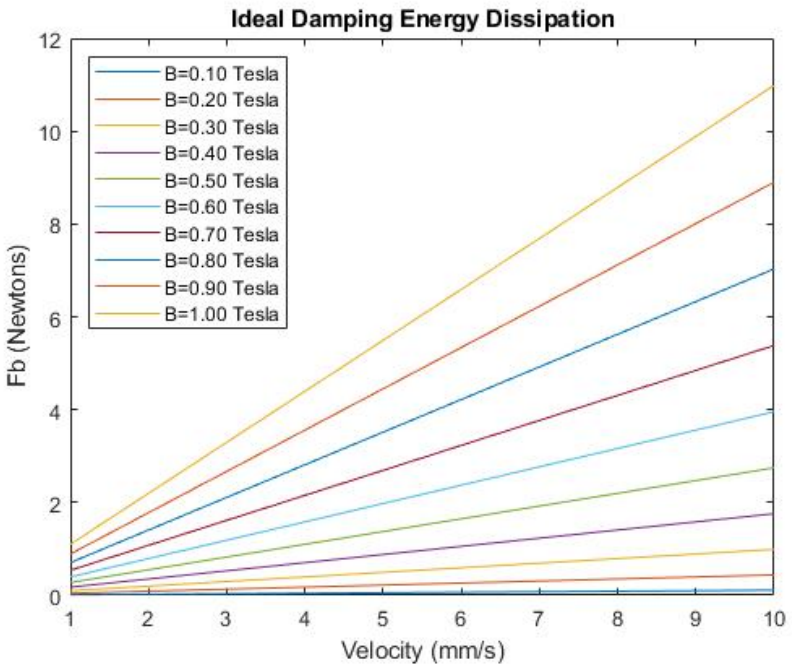

Figure 3.28: Ideal Damping Energy Dissipation with varied Magnetic Field Strength

The slope of each line can then be graphed against the strength of the magnetic field.

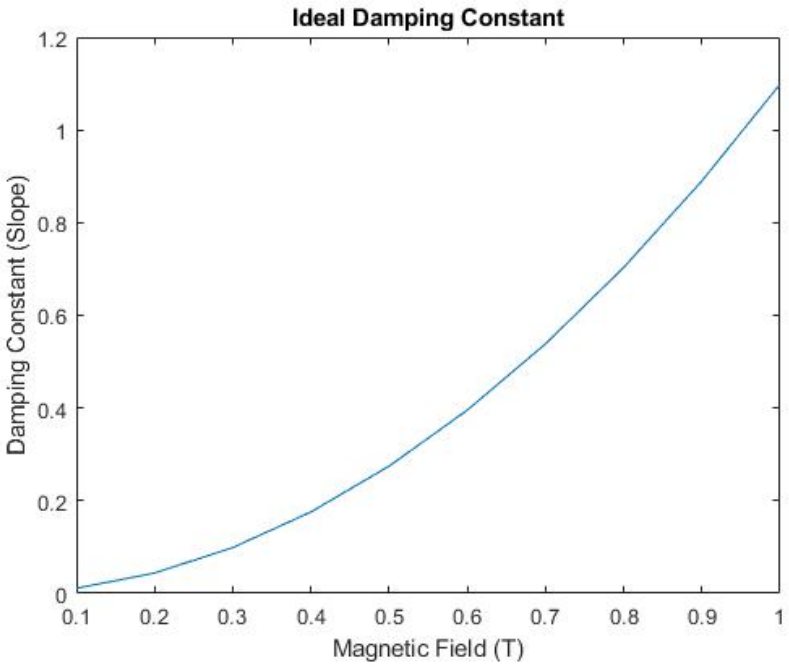

Figure 3.29: Ideal Damping Constant Ns/m

The slope of the damping constant as a function of magnetic field strength (T) is:

$$b = 1.0987B^2 + 7e^{-15}B - 6e^{-15} \tag{3.4}$$

Magnetic Field (Tesla)	Damping Constant
0.1	0.010986694
0.2	0.043946775
0.3	0.098880244
0.4	0.175787101
0.5	0.274667345
0.6	0.395520977
0.7	0.538347996
0.8	0.703148403
0.9	0.889922198
1	1.09866938

Figure 3.30: Ideal Damping Constants Ns/m

Going back to the second order underdamped analysis after determining the

range of damping constants:

$$
\begin{aligned}
w_n = \sqrt{a_0} &= \sqrt{\frac{2k}{I}} \\
\zeta = \frac{a_1}{2w_n} &= \frac{\frac{b}{I}}{2\sqrt{\frac{2k}{I}}} \\
2\zeta w_n &= \frac{b}{I} \\
I &= \frac{b}{2\zeta\sqrt{\frac{2k}{I}}} \\
I &= \frac{b^2}{8k\zeta^2}
\end{aligned}
\tag{3.5}
$$

w_n = natural frequency, ζ = damping ratio

Using this final equation we can predict the range of moment of inertia's that can be damped using a magnetic field of $0.1 - 1(T)$ and a damping ratio of $0.4 < \zeta < 0.8$.

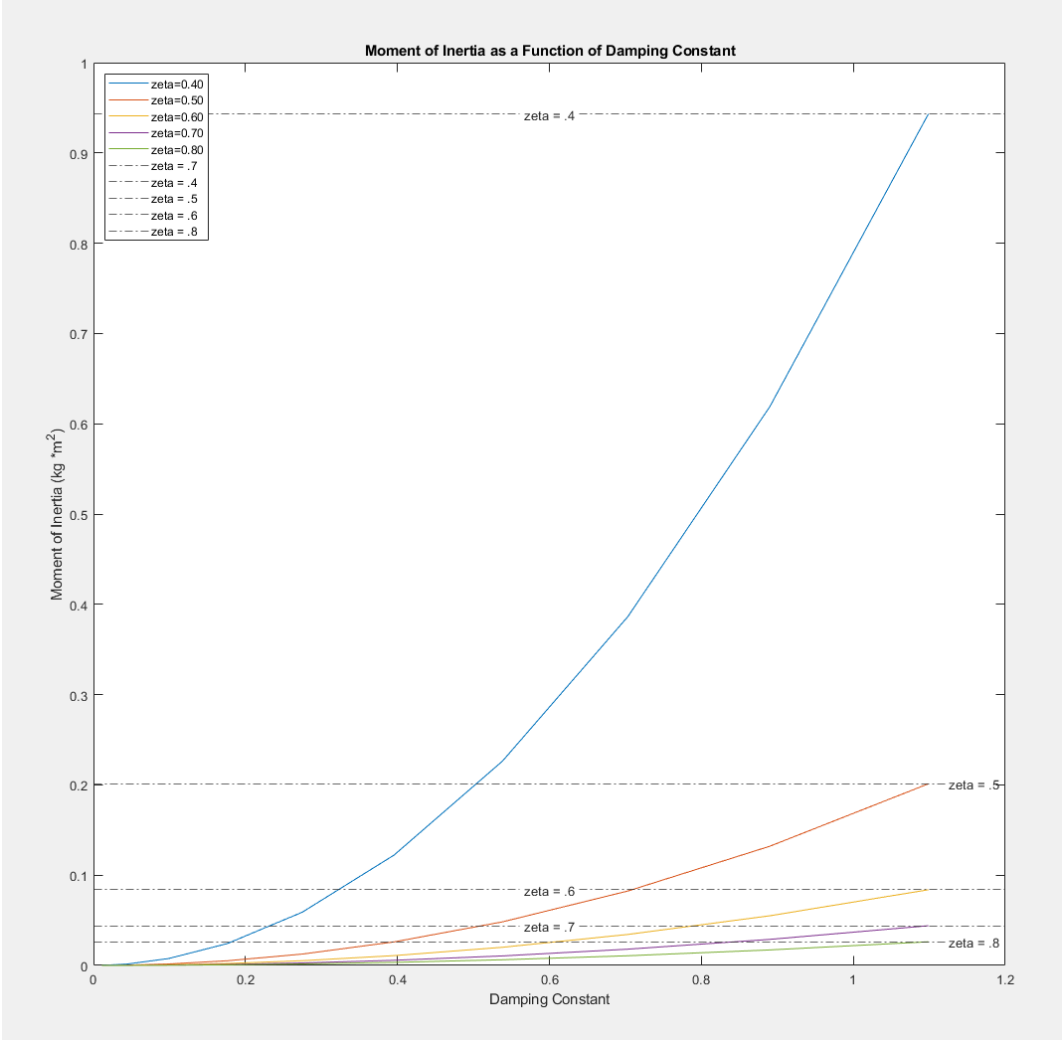

Figure 3.31: Moment of Inertia as a Function of Damping Constant

Zeta	Max Moment of Inertia kg m^2
0.4	0.94302688
0.5	0.201179068
0.6	0.083824612
0.7	0.043989592
0.8	0.026195191

Figure 3.32: Maximum Moment of Inertia for a selected Damping Ratio

The selected copper plate coupled when mounted on the bare torsional arm will have a moment of inertia of 0.02428 $kg * m^2$ through the Y (vertical) axis. This is a CAD approximation of Figure 3.33 shown below.

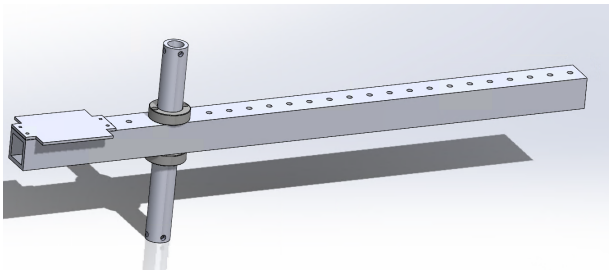

Figure 3.33: CAD Bare Torsional Arm

This moment of inertia is small and is not restricted by any ζ values. Once the torsional arm is complete with a thruster, thruster mount plate, and corresponding counter weight it may not be able to use a value of $\zeta = 0.8$. Returning to the second order system equation we can approximate the required magnetic field strength from the ζ, k (21.1103 Nm/rad a property of the flexure pivots used), the dimensions of the copper plate (3.175mm thick, .005806 m^2 area) and moment of inertia. This will be used to predict the size of the permanent magnet required.

$$\begin{aligned} 2\zeta w_n = \frac{b}{I} &= \frac{\sigma \delta S B^2}{I} \\ 2\zeta\sqrt{\frac{2k}{I}} &= \frac{\sigma \delta S B^2}{I} \\ B &= \sqrt{\frac{2I\zeta\sqrt{\frac{2k}{I}}}{\sigma \delta S}} \end{aligned} \tag{3.6}$$

Solving the above equation for the range of ζ values leads to:

Zeta	Magnetic Field (Tesla)	Damping Constant
0.4	0.027152183	0.809984165
0.5	0.030357064	1.012480206
0.6	0.033254497	1.214976247
0.7	0.035918962	1.417472289
0.8	0.038398986	1.61996833

Figure 3.34: Approximate Required Magnetic Field for selected ζ value

The damping constant and moment of inertia values can be plugged back in to the second order damping equation. The entire equation can then be analyzed using Matlab's Step command for approximate damping performance.

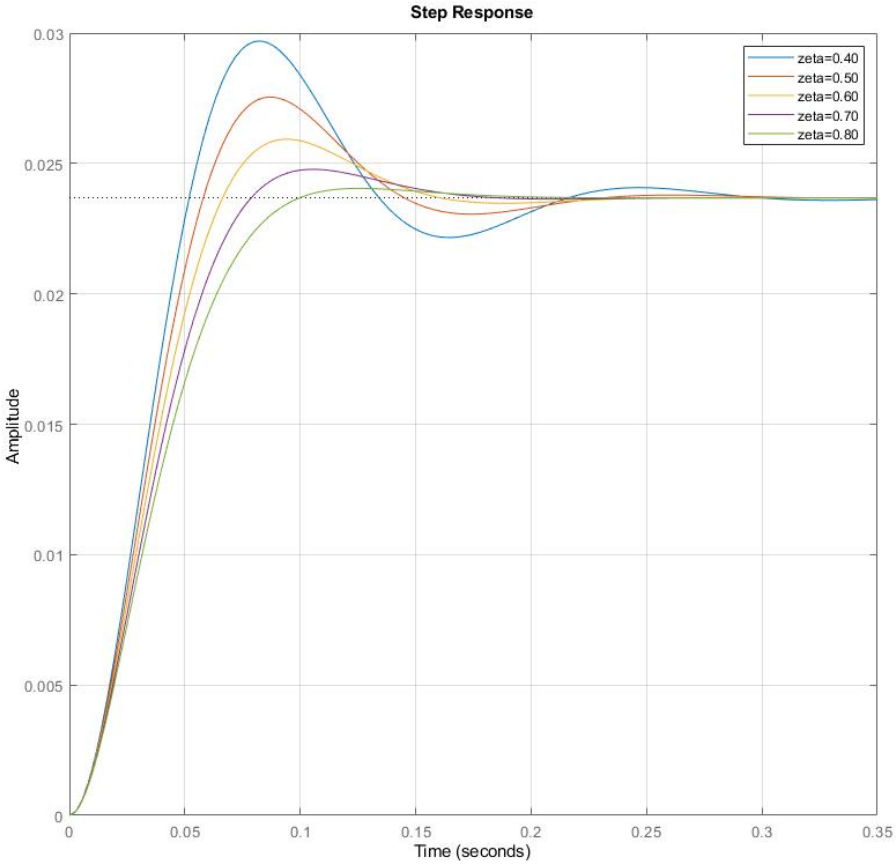

Figure 3.35: Response of $\frac{\theta(s)}{\tau_T(s)}$ to Unit Step Input

Using the information gathered from Figure 3.18 a $\frac{9}{16}$" OD by $\frac{3}{8}$" thick cylindrical Neodymium grade N52 permanent magnet was selected. The approximate cost of this magnet was $10.00. The magnetic field was mapped using the procedures listed within Chapter 4: Testing and Validation. The results of that testing will be displayed below.

Three mapping runs were completed with nearly identical results. The runs were then averaged into a single line map. Setting a trend line to this data was problematic. A third order polynomial is consistent with the field data the smaller the distance, it however has 2 local max/mins between $10 - 20mm$. The reverse is true of the exponential trend line. The generated exponential function under predicts at small distances but closely mimics the field drop off as the distance increases.

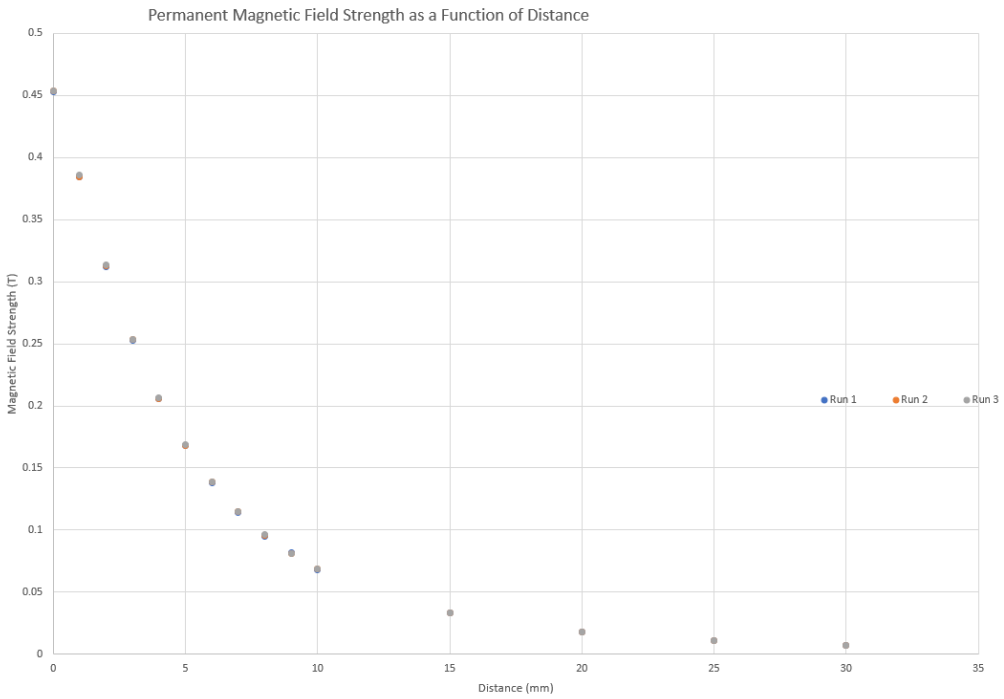

Figure 3.36: Magnetic Field Strength as a Function of Distance

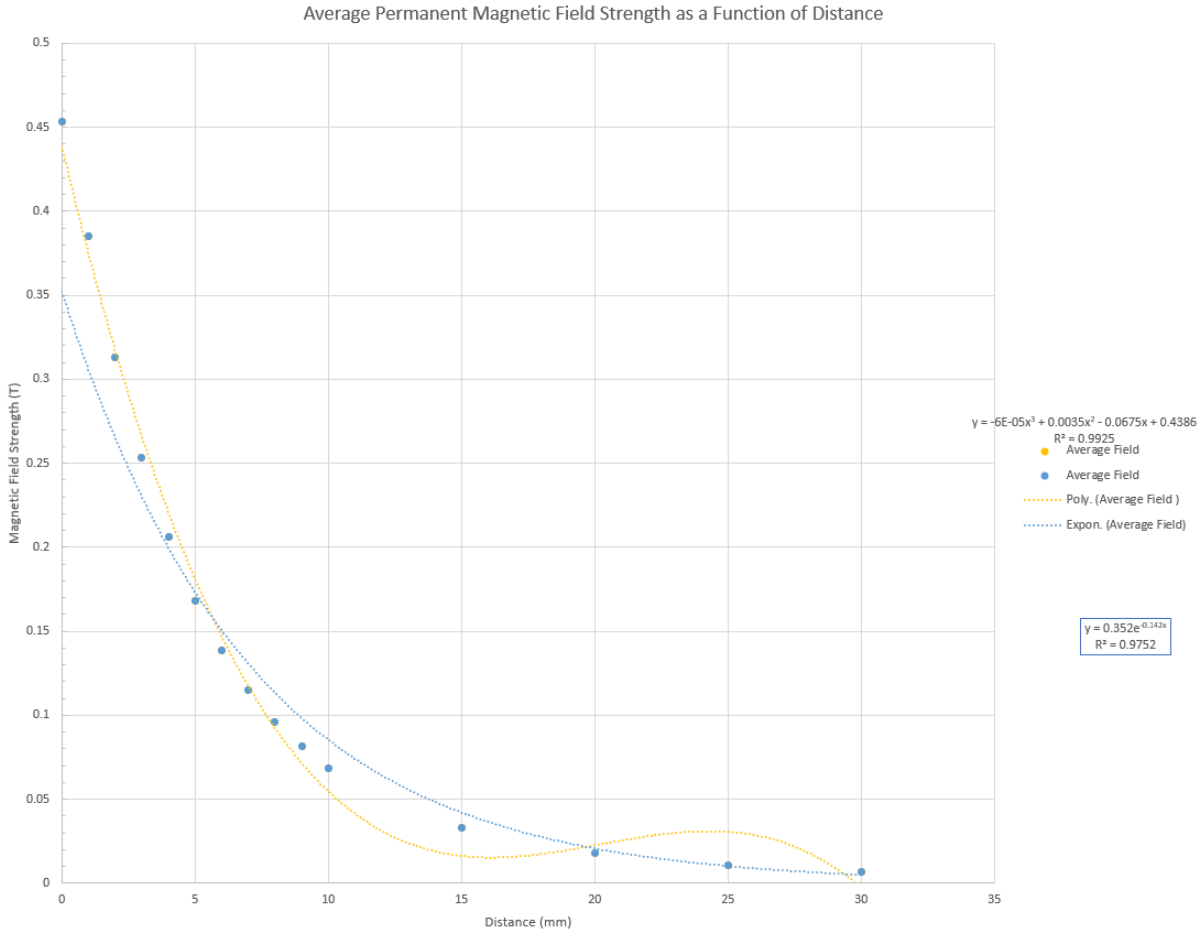

Figure 3.37: Average Magnetic Field Strength as a Function of Distance

The magnet selected above provides a much stronger magnetic field than the one predicted to be required. This was intentional to provided additional flexibility to accommodate various thrusters and to make up for many of the modeling approximations used. The magnet can always be set farther from the copper plate if a lower strength magnetic field is required.

To make the task of setting up the magnet distance simpler a short Matlab script was written. This requires the input of the magnetic field required (in Tesla) and then uses either the polynomial or the exponential curve to determine the distance. 0.09 Telsa was the point where the equations are swapped. This is not a perfect solution but this ballpark figure will make the initial set distance less time consuming. The output of this script is rounded to the nearest mm.

```
%Permanent Magnet Initial Distance Setup
%Jeremy Baiocchi
clear all; close all; clc
%Magnetic Field required
prompt = "What is the Required Magnetic Field value in Tesla? "
B = input(prompt);
syms x
if B <.09
    eqn = B == .352*exp(-.142*x);
else
    eqn = B == -6*10^(-5)*x^3+.0035*x^2-.0675*x+.4386;
end
S = solve(eqn,x,'real',true,'MaxDegree',4);
format compact
display('Magnet Set Distance Rounded to nearest whole number')
D = round(double(S))
display('mm')
```

Figure 3.38: Permanent Magnet Distance Setup

To support the permanent magnet, a piece of delrin was machined to slide along an L bracket made of aluminum. A pair of screws provide the clamping force to maintain the set height adjustment. The delrin had a recess drilled into one end for the magnet. Two lateral holes were drilled for a pair of set screws to prevent the magnet from falling out. The resulting magnet support is capable of bolting directly to the thrust stand base for use without a linear stage. Also, it can be bolted to a linear stage for height adjustment within the chamber. Small alignments holes were added to allow to graduated steps manually if used without a linear stage. These close tolerance holes ended up being too difficult to machine to the precision required, and were omitted. They are still shown on the CAD drawings under Appendix A.

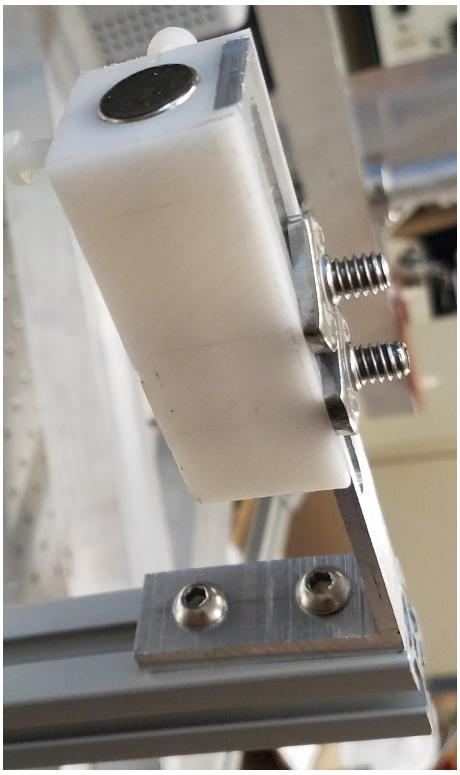

Figure 3.39: Magnet Support Slide

3.3.8 Linear Stage

To retain damping adjustability when the vacuum chamber is sealed, a linear stage was used to move the magnet closer or farther away from the copper plate depending on the operator's need. The existing L-bracket was attached to an arm extending from the linear stage. This prevented a second mounting solution from being required. The added height of the linear stage arm would restrict the distance the magnet could be moved. The damping system refitted to the top of the torsional arm to provided the necessary space for the linear stage to move.

The linear stage used was a BiSlide MN10-0100-E01-21. This model has an advance per step of .00025 in ($6.35e^{-06}m$). each millimeter of travel would require 158 turns. The stepper motor was controlled using a Velmex VXM Stepping Motor Controller. Provisions for these devices within the vacuum chamber was already set up and was convenient to setup and use. Detailed instructions on how to use the linear stage will be explain in Chapter 4: Testing and Validation. [**19**]

Figure 3.40: Magnet Support Slide attached to Linear Stage

Figure 3.41: Velmex VXM Stepper Motor Controllers

3.4 Budget

Although our budget resections are limited due to funding from the SWARM-EX CubeSat team, a projected budget can be seen in Table (3.6).

System	Component	Quantity	Cost	Subtotal
Flexure	I-30Flexure Pivots	2	$221.04	**$221.04**
Optical Displacement	muDMS-64 Sensor	1	$1,445.00	
	Bv133 Vacuum Passthru	1	$1,845.00	
	LT1 Translation Stage	1	$396.06	
	PTFE Cable Jacket	1	$200.00	
	18' Fiberoptic Cable	1	$225.00	
	1/4" SS Target Disc	1	$30.00	
	1/2" SS Target Disk	1	$55.00	
	18" 6061 Aluminum	1	$29.48	**$4,225.54**
Leveling	ADIS16209/PCB	1	$112.00	
	SM-25 Micrometer	2	$270.00	
	3/8 - 40 Tap	1	$30.00	
	9.5" Aluminum Beam	1	$16.55	**$428.55**
Damping	Macor Cylinder	1	$131.20	
	Insulated Wire Spool	1	$150.00	
	Copper Plate	1	$30.00	
	L brackets	6	$25.00	
	Attaching Harware	14	$30.00	
	Spacers	4	$20.00	
	Iron Core	1	$35.00	**$421.20**

Total	**$5,296.33**

Table 3.8: Estimated Budget

3.5 Facilities

The main facilities that will be used for completion for this project will be the Aerospace Laboratory for Plasma Experiments on the WMU CEAS campus and the student project laboratory as required.

Chapter 4

Testing and Validation

4.1 Fiberoptic Displacement Sensor

The main objective of this validation is to ensure that the optical sensor produces accurate and precise measurements which are necessary for the operation of this thrust stand.

4.1.1 Testing Startup and Configuration

1. Connect the D64 optical sensor to the AC/DC power adaptor
2. Use the USB adaptor cable to establish a connection between the sensor and PC.
3. Turn on the power to the power adaptor by plugging into three-prong wall outlet.
4. Open Philtec DMS Control Software on PC (must be loaded onto computer for first use).
5. Select the desired sensor serial number from the Com Port menu on the Standard channel tab.
6. Select "Open Com Port"
7. Click on the Configuration tab
8. Set the Temperature of the electronics to the steady state temperature and allow 10-15 minutes for electronics to reach thermal equilibrium. Then adjust the setpoint temperature to 3°C above the unheated steady state temperature.
9. Set the Sampling Rate to 2.54 samples/second which is best for slow speeds.
10. While moving the muDMS-D64 within it's operating range of 6mm adjust the Transmit Power so that the peak value of the receive signal does not exceed 95 percent
11. Click "Peak Hold" while moving the sensor within its range and reach the highest reflectance value.

4.1.2 Testing Equipment

1. muDMS-D64 Fiber Optic Displacement Sensor (1 pc.)
2. AC/DC Power Source (1 pc.)
3. Locking USB Cable (1 pc.)
4. 5/32 in. and 3/16 in. Allen Wrench (1 pc. each)
5. Seven (7) appropriate length screws 80/20 compatible
6. DDSM100 Direct Drive Stage (1 pc.)
7. 2x2 80/20 plates
8. 80/20 Extrusion (1 pc.)
9. Right Angle 80/20 Frame
10. 80/20 Bread Board

Figure 4.1: Optical Sensor Photograph

Figure 4.2: AC/DC Power Supply and USB Cable

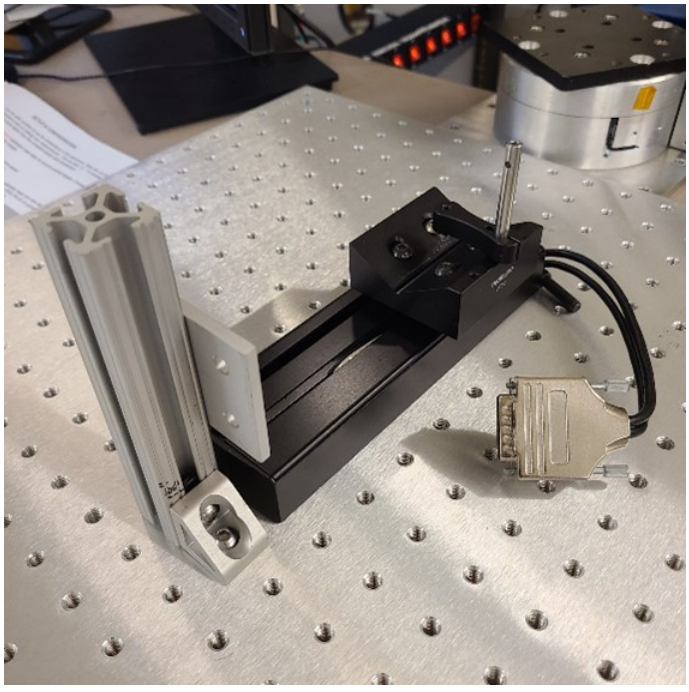

Figure 4.3: DDSM100 Linear Drive Stage on 80/20 Bread Board

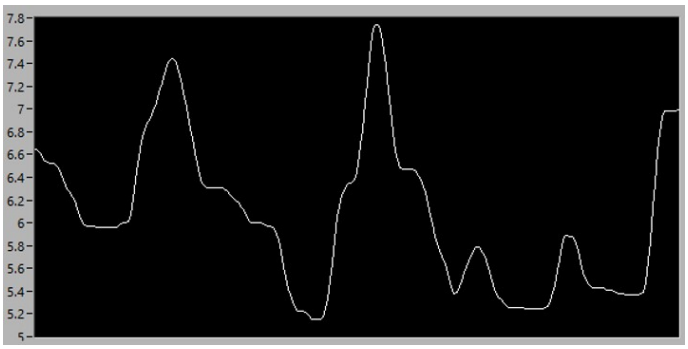

Figure 4.4: Optical Sensor Displacement Test Output (mm vs. time) in Philtec DMS Control Software

This figure above shows a sample of the data obtained during testing and validation of the Optical Displacement Sensor and the associated DMS Software that outputs the displacement data. This information was validated using a set of calipers to ensure accuracy. Since the sensor is accurate within the thousandth of an inch, it is much more precise than hand measurements. Therefore, the calipers were used simply to validate the reported data was reasonable. Manual measurements were within +/- 0.5mm to the sensor. This was concluded to be acceptable and validates the sensors capabilities. To accurately calculate thrust, a LabView VI must be created to interpret the reported displacement and use the known arm length and torsional spring rates for said calculations. This responsibility falls outside the scope of this subsystem and report. However, it is being worked on by WMU undergraduate and graduate researchers at the time of writing this report.

4.2 Leveling

The purpose of this validation testing was to test the basic setup and use of the Analog Devices Digital Inclinometer and Accelerometer and be able to clearly communicate the setup for future work and integration into the thrust stand.

4.2.1 Test Equipment

ADIS16209 The inclinometer sensor used for the system.

Arduino Due The microcontroller used was the Arduino Due. This was chosen because of the 3.3v logic level for the SPI port and also familiarity. The pinouts for the Arduino Due is in figure (6), however a majority of the pins used are the ones located on the SPI region, (not to be confused with ICSP at the top of the board). The programming USB jack was used for all the programming.

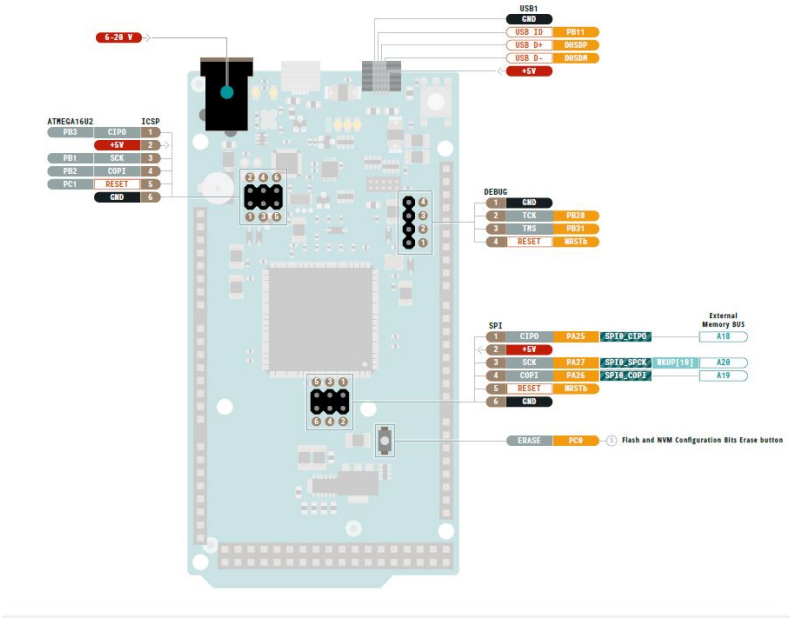

Figure 4.5: Arduino SPI Pinout (Courtesy of Arduino)

4.2.2 Setup Procedures

1. Setup the proper connections as listed below and identified in figure (4.6) and (4.7).

   (a) ADIS16209 CS (J1 – 3) to Arduino Due GPIO 5

   (b) ADIS16209 SCLK (J1 – 2) to Arduino SPI SCK

   (c) ADIS16209 DIN (J1 – 4) to Arduino SPI MOSI

   (d) ADIS16209 DOUT (J1 – 6) to Arduino SPI MISO

   (e) ADIS16209 GND (J1 - 8) to GND on Power Supply and/or Arduino GND

      i. NOTE: If power is being run from Arduino only, the ground can only go to the Arduino. If power is coming from the power supply, then a ground must be connected to the Arduino and the power supply.

   (f) ADIS16209 VDD (J1 – 10) to 3.3 V from Power Supply or Arduino

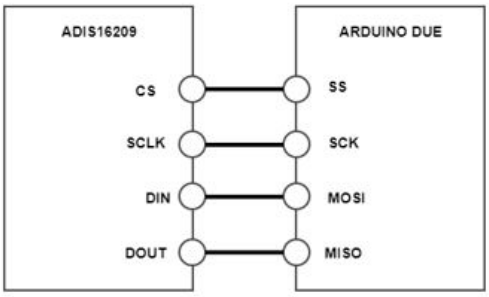

Figure 4.6: ADIS16209 Experimental Pinouts

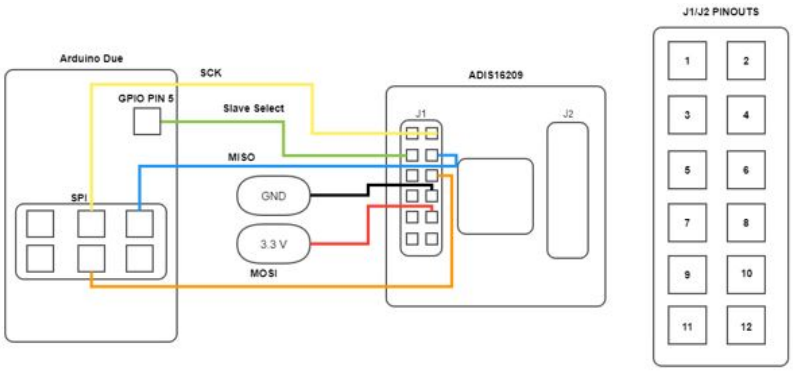

Figure 4.7: Experimental Setup Lines

2. If using a power supply, limit the current appropriately (normal mode draws between 11 and 14 mA), and set the voltage to 3.3V.
3. Plug in the Arduino through the programming port with micro USB to a computer with both the Arduino IDE and the SPI code downloaded
4. Run the code to see the output data
5. Edit the code to preferred outputs/timings

4.2.3 Results

The code was ran and the ADIS16209 consistently returned expected result of inclination. An oscilloscope was connected to the SPI communication leads to see the wave patterns.

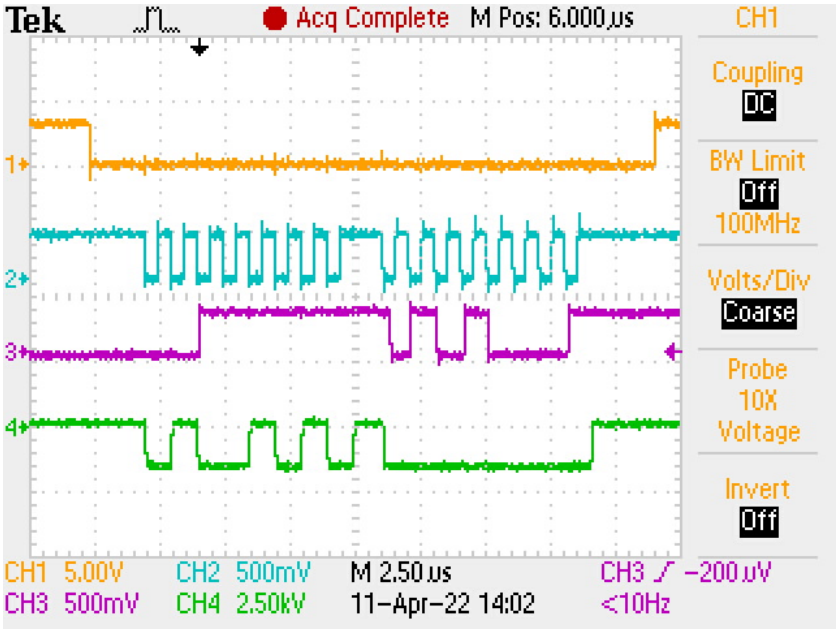

Figure 4.8: Oscilloscope Data from ADIS16209

The code for the inclinometer is currently being added to system Labview for full system integration.

4.3 Damping System

4.3.1 Magnetic Field Measurements

Magnetic field measurements were completed using a Lakeshore model 425 gauss meter using the following procedure.

1. Restrain gauss meter probe near testing are.
2. Move magnet far away from probe.
3. Turn on and zero gauss meter to remove background field interference.
4. Restrain magnet to linear stage.
5. Position linear stage with magnet as close to end of gauss meter without touching, ensure gauss meter is centered on magent face.
6. Record magnitude of magnetic field
7. Step linear stage away from probe desired distance.
8. Repeat Steps 6 and 7 as required.

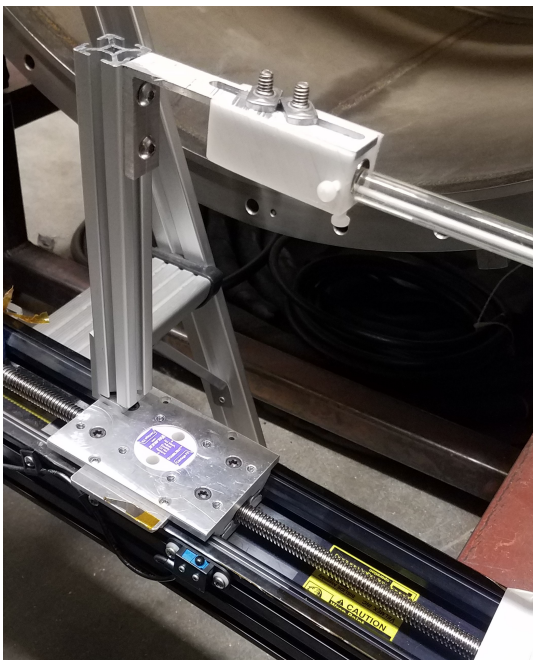

Figure 4.9: Permanent Magnetic Field Testing

4.3.2 Linear Stage Operation

Linear stage movement is controlled by providing inputs to a VI which outputs the movements to a stepper motor controller. The BiSlide model MN10-0100-E01-21 used for this project has an advance per step of .00025 in ($6.35e^{-06}m$). The VI requires distance inputs in the form of step numbers. The real unit step number can be calculated using the following:

$$\frac{Distance}{Advance\ per\ step} = Steps\ [\mathbf{18}] \tag{4.1}$$

For example: 1 mm of travel is 158 steps. The command input lines reads: C,I1M158,R. C = clear all commands, I1M = selects motor to step (this may change depending on which port the motor is plugged into), 158 = 158 steps (if this value is positive and will move away from the motor, with a negative prefix the stage will move towards the motor), R = Run. [**18**]

This is a short list of commands and their explanations, before using the motor controller it is highly recommended to read the Velmex VXM Stepper Motor Controller User Manual. [**18**]

1. Attach extension arm to linear stage.
2. Rigidly install linear stage so the stage extension arm is centered above copper plate.
3. Connect and secure motor and stage electrical connections.
4. Turn on VXM Stepping Motor Controllers, wait for On-Line lights to illuminate.
5. Optional: Use Jog switches to roughly position extension arm closer to copper plate.
6. Attach magnet support bracket to extension arm.
7. Set lower stage proximity switch to prevent contact between magnet and copper plate.
8. Open "AHC32_TableMove.vi", ensure input setting match the figure shown below.
9. Using the following commands lower magnet until it is nearly in contact with the copper plate, adjustment of the proximity switch may be required to reduce distance.
10. Stage Up (Towards the motor): C,I1M-158,R (1mm increments)
11. Stage down (Away from motor): C,I1M158,R (1mm increments)
12. Once a "zero" is established ensure proximity switch makes contact with stage at zero point.
13. Use step 10 & 11 commands to position the stage for testing as required, the step distance can be modified if desired.

It is highly recommended that all movements made to the stage are recorded in a log. There is no vertical height feedback from the stage, and if distance to the copper plate is unknown the stage must be send down to the zero proximity switch and then walked up to its required testing distance. It is vital that the lower proximity switch is set properly to prevent damage to equipment during any down movement commands.

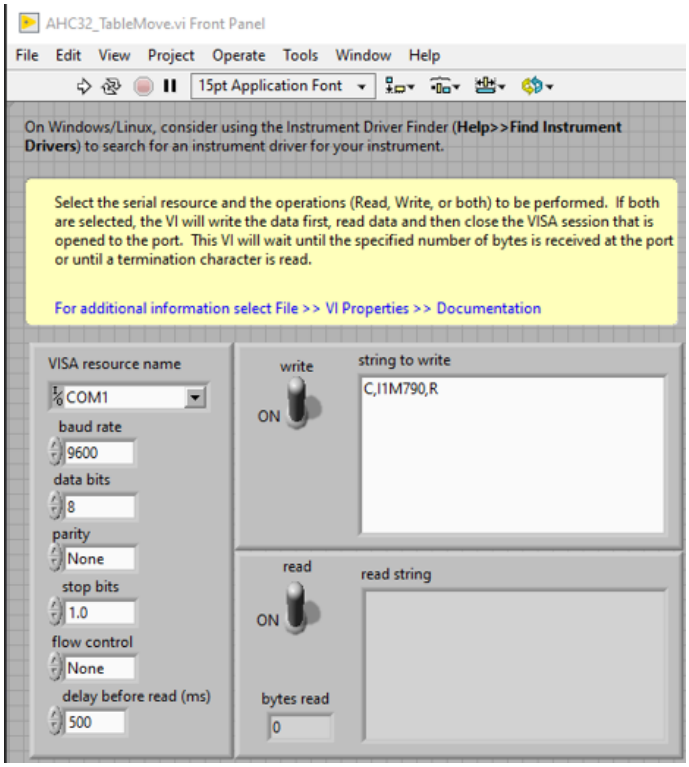

Figure 4.10: AHC32_TableMove.vi input settings

Figure 4.11: Mounted Damping system

4.3.3 Damping System Testing

System testing was completed by placing the assembled thrust stand in the vacuum chamber. The thrust stand was leveled and the optical sensor and damping systems were set up. The calibration system is not complete and ready for testing yet. The

torsional arm was bare without counter weights,thruster mount plate, or thruster. For these tests the magnetic distance was set at 4mm, 0.206 Tesla. Motion was induced into the torsional arm by deflecting the thruster side of the arm. This is not ideal, without the application of a known force it is not possible to take a detailed look at the results. It did allow recording of initial damped and undamped testing. However, this data can be used to extract relative velocity data from the system.

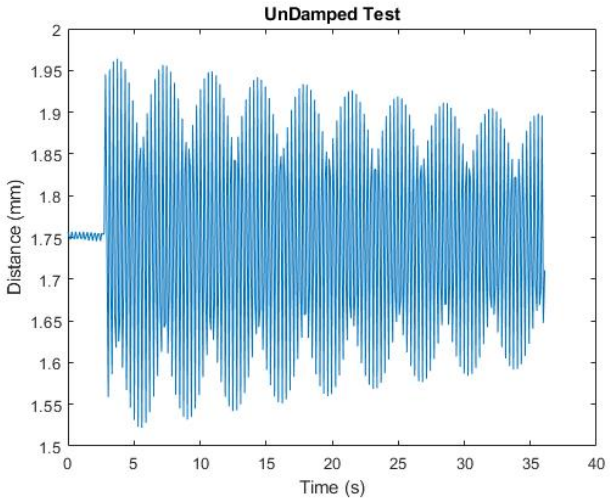

Figure 4.12: Undamped Test

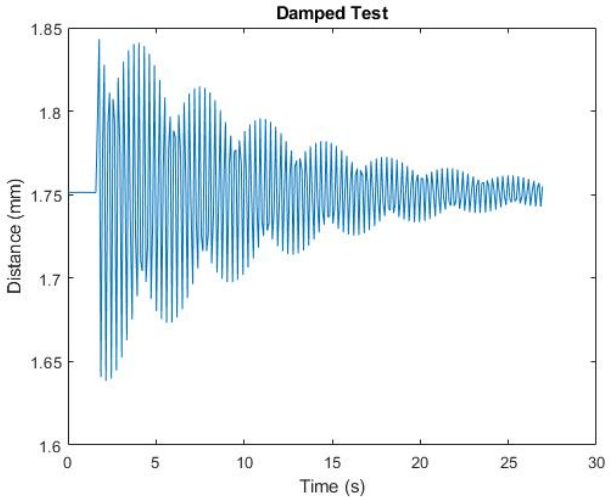

Figure 4.13: Damped Test

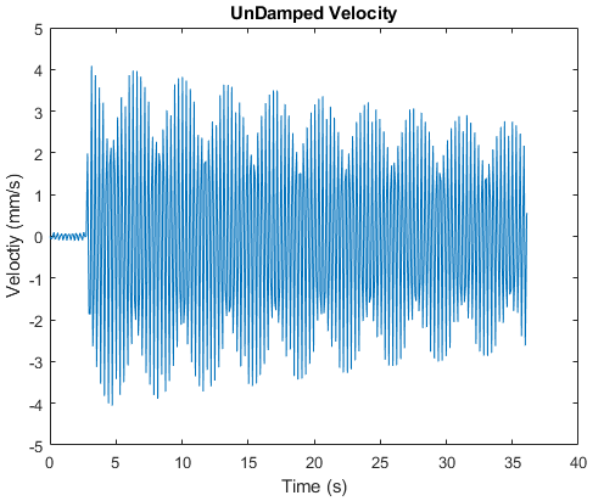

Figure 4.14: Undamped Velocity

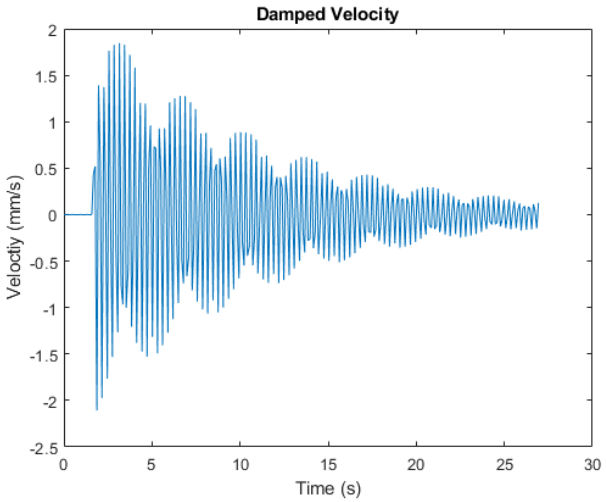

Figure 4.15: Damped Velocity

There are a few conclusions we can draw from this data. The damping system is working, without the application of a know force it is not possible to analyze the specifics beyond that. The damping system appears to be under performing, the magnetic field used for testing was much stronger than what was predicted to be required and took roughly 22 seconds to reach steady state. This trend is not acceptable and if testing with a known force confirms this initial result the damper will need to be made stronger. Initial velocity data is close to predicted levels of vibration.

Currently it is a struggle to use the Philtec DMS recording function. This growing pain should resolve itself with more testing sessions and a streamlined VI. The save file format is a text file with many unnecessary columns. Due to the unique time stamp format, data currently has to be manually manipulated into a form Matlab can import, greatly increasing the time required to analyze data. This unique time stamp format also made data runs longer than 1 minute difficult to import. This time stamp issue is not expected to Once the calibration system is ready, more

detailed experimental testing can commence to confirm if this damping solution is viable or if adjustments need to me made.

Chapter 5

Conclusion

5.1 Current Progress and Future Works

5.2 Conclusion

A Thrust Stand is a device that uses basic physical properties of torsion and displacement to experimentally measure and calculate the thrust measured by an Electric Propulsion Thruster. Electric Propulsion Thrusters are small propulsion devices that produce between 10^{-6} Newtons to 10^{1} Newtons. These small thrusters are utilized by light spacecraft, such as satellites, due to their high efficiency at low thrust levels. A Thrust Stand must be used to measure the thrust generated by an Electric Propulsion Thruster experimentally. Since these thrusters operate in vacuum environments, the thrust stand must also be made of vacuum-rated materials to avoid outgassing.

Three organizations at Western Michigan University all work with electric propulsion thrusters without proper methods of obtaining direct experimental data. These organizations are: WMU's Aerospace Laboratory for Plasma Experiments (ALPE), Western Aerospace Launch Initiative (WALI), and WMU's involvement with Space Weather Atmospheric Reconfigurable Multiscale Experiment CubeSat (SWARM-EX). This Torsional Thrust Stand will perform experimental thrust measurements for all three organizations inside the High-Vacuum (10^{-7} - 10^{-3} Torr) Chamber inside the ALPE Lab. Additionally, this modular design will allow for relatively easy replication of the thrust stand for other groups in need of direct thrust measurements.

The Four systems of the Torsional Thrust Stand that are within the scope of this proposal are the Flexure, Optical Displacement, Leveling and Dampening Systems. The Flexure System uses two I-30 Flexure Pivots to allow the torsional arm to rotate with a known spring constant. The Optical Displacement System uses a muDMS-64 Fiber Optic Displacement Sensor to measure the linear displacement of the torsional arm. This is mounted on the 80/20 breadboard inside the path of displacement. The Leveling System uses strategically located micrometers, mounted underneath the base of the entire stand, to level the system quickly and accurately. The Damping System uses permanent magnet dampeners on the linear stage to limit noise and other types of internal and external interference that could alter data collection. The total cost of these systems is estimated to be $5,296.33 USD.

5.3 Engineering Impact

5.3.1 Global

Satellites are used to connect the global community. A thrust stand is a method to improve the development of the propulsion of these satellites. More refined propulsion could result in improved lifetime and performance of satellites for various purposes such as international communication.

5.3.2 Economic

A successful completion of the thrust stand allows the groups at WMU and economical and convenient way to produce test results for their thrusters. Additionally, this modular design allows other groups in need of a thrust stand to easily adapt these design choices of this thrust to replicate their own in a cost-effective manner.

5.3.3 Environmental

The modular design and use of components off the shelf allowed for minimal waste to be produced.

5.3.4 Societal

Electric propulsion solutions will continue to be developed for space applications and many more advances in the technology are expected as time goes on. A project like this allows for the proper development of these thrusters which have already cemented a permanent spot in aerospace.

5.4 Future Works and Recommendations

Many things can be learned from this project that are applicable for future groups to consider. The first recommendation is to have a point of contact who expresses expertise in each system used. Since each system in the thrust stand are incredibly unique from each other, not much mutual knowledge is shared between them. Damping system performance needs to be investigated further when the calibration system is ready. Additionally, with further funding the leveling system could be improved to have motorized actuation to allow for more convenient leveling. A final recommendation is to allow a feasible timeline. Many times during this project timeline, progress was slowed due to delivery times or machining progress. It would be wise to prepare with ample time for building the systems of a thrust stand.

5.5 Acknowledgements

Our Senior Design group would like to thank Western Michigan University's College of Engineering and Applied Sciences for the education provided while attending. Additionally, we would like to especially thank our faculty advisor, Dr. Kristina Lemmer for the opportunity to work on this project and for encouragement and guidance throughout this process. Hannah Watts, a graduate student, has also

provided us with fantastic guidance and knowledge necessary to achieve our goals. Additionally, Mohammad Asif contributed to our success by being a mentor and overseeing project completion. Tom Kerber was responsible for helping with machining as well as technicians as Mann+Hummel Inc. Allin Kahrl provided machining insight and help with part fabrication. Also, thank you to Austin Tomas for his patience and handling of SWARM-EX communication. Another thanks is in order to the SWARM-EX cubesat team for providing funding, and in extension, the National Science Foundation. Thank you to Phoenix Wire for providing low-outgassing insulated magnetic-wire. A thanks is in order for Dr. Bade Shrestha for instructing the ME/AE4800 course. Lastly and very importantly, we would like to thank the Allwine, Baiocchi, and Hefferan families for their endless support as well as dear friends. Everyone mentioned is responsible for aiding in the success of this project and only the surface of their impact can be seen through this paper. Thank you to you all.

Bibliography

[1] Analog Devices. (2019) High Accuracy, Dual-Axis DIgital Inclinometer and Accelerometer - ADIS16209 Data Sheet. Retrieved Janurary 20, 2022, from https://www.analog.com/en/products/adis16209.htmlproduct-overview

[2] Callaghan, E. E., & Maslen, S. H. (1960). THE MAGNETIC FIELD OF A FINITE SOLENOID. NASA Technical Note (TN) D-465. Document ID: 19980227402

[3] C-Flex, Pivot Bearing Guide. Retrieved November 20, 2021, from https://c-flex.com/pivot-bearings/design-guide/

[4] Ding, C., & Cheng, M. (2016). The measurement of low impulse from pulsed electromagnetic thrusters by thrust stand. Proceedings of the 2016 7th International Conference on Mechatronics, Control and Materials (ICMCM 2016). https://doi.org/10.2991/icmcm-16.2016.23

[5] Goebel, D. M., & Katz, I. (2008). Fundamentals of electric propulsion ion and hall thrusters. Wiley.

[6] Kokal, U., & Celik, M. (2017). Development of a mili-newton level thrust stand for thrust measurements of electric propulsion systems. 2017 8th International Conference on Recent Advances in Space Technologies (RAST). https://doi.org/10.1109/rast.2017.8002970

[7] Lemmer, K. (2017). Propulsion for CubeSats. Acta Astronautica, 134, 231–243. https://doi.org/10.1016/j.actaastro.2017.01.048

[8] Lerner, L. (2011). Magnetic field of a finite solenoid with a linear permeable core. American Journal of Physics, 79(10), 1030–1035. https://doi.org/10.1119/1.3602096

[9] Liu, R. & Bu, H. (2013). Design on LVDT Displacement Sensor Based on AD598. Sensor & Tranducers, 21(3), 68-73. http://www.sensorsportal.com

[10] Lu, X., Zhang, Q., Weng, D., Zhou, Z., Wang, S., Mahin, S. A., Ding, S., & Qian, F. (2016). Improving performance of a super tall building using a new eddy-current Tuned Mass Damper. Structural Control and Health Monitoring, 24(3). https://doi.org/10.1002/stc.1882

[11] Philtec Inc. (2019) D Model Sensors - Reflectance Dependent. Retrieved January 8, 2022, from https://philtec.com/products/d-model-sensors-reflectance-dependent/

[12] Philtec Inc. About the Sensors, Retrieved November 10, 2021, from https://philtec.com/about-the-sensors/

[13] Polk, J. E., Pancotti, A., Haag, T., King, S., Walker, M., Blakely, J., & Ziemer, J. (2017). Recommended Practice for Thrust Measurement in Electric Propulsion Testing. Journal of Propulsion and Power, 33(3), 539–555. https://doi.org/10.2514/1.b35564

[14] Sandwell, G. (2020, February 14). Learn About Vibration, Volume 1. Vibescorp.Ca. Retrieved January 10, 2022, from https://www.vibescorp.ca/learn-about/basic-understanding-of-machinery-vibration/

[15] Serway, Raymond A. (19861983). Physics for scientists & engineers with modern physics. Philadelphia :Saunders College Pub.

[16] Robertson, W., Cazzolato, B., & Zander, A. (2012). Axial Force between a thick coil and a cylindrical permanent magnet: Optimizing the geometry of an electromagnetic actuator. IEEE Transactions on Magnetics, 48(9), 2479–2487. https://doi.org/10.1109/tmag.2012.2194789

[17] Wang, J. Z., Bian, X., Li, Q., & Wu, J. H. (2020). A magnetic damper for low temperature. AIP Advances, 10(10), 105107. https://doi.org/10.1063/5.0018572

[18] Watts, Hannah, "Design of a Thrust Stand for Electric Propulsion" (2019). Honors Theses. 3090. https://scholarworks.wmich.edu/honors_theses/3090

[19] Velmix,INC, (2004, December 29). VXM Stepping Motor Controller User's Manual (Extended Version) Model VXM-1,2,3,4. Document number VXM:-UM-E5

Appendix A

A.1 Requirements Verification Matrix

Maturity	
High	This requirement is finalized and no longer needs further revisions and is clearly explained and can be used to drive design considerations.
Medium	This requirement is on the correct path of becoming finalized, however still needs revisions in order to express complete clarity.
Low	This requirement needs extensive revisions and rewording in order for clear design direction.

Figure A.1: Requirements Verification Matrix Maturity Levels

ID	Maturity	Source	Statement	Verification Method	Comments
Objective Statements					
OBJ-1	High	N/A	Design the flexure, optical sensing, damping and leveling systems for an electric propulsion thrust stand to be used to measure low thrust devices	N/A	
OBJ-2	High	N/A	Contribute documentation to electric propulsion academic community for a low cost option for thrust measurement	N/A	
System Requirements					
SYS-1	High	OBJ-1	The entirety of the thrust stand shall be able to fit and operate in Aerospace Laboratory for Plasma Experiement's 1.5 meter long with 1 meter diameter vacuum chamber	Inspection	
SYS-2	High	SYS-1	The thrust stand shall be compatable with internal 80-20 extrudeded aluminum structure within the vacuum chamber	Demonstration	
SYS-3	High	SYS-1	The systems of the thrust stand shall be vacuum compatable with little to no outgassing	Demonstration	
SYS-4	High	SYS-1	The systems of the thrust stand shall be compatable with connections and feedthroughs	Demonstration	
SYS-5	Medium	OBJ-2	The thrust stand shall have simple elements that can easily be machined and assembled	Demonstration	
SYS-6	High	OBJ-1	The thrust stand shall have a resolution of 1 μN	Analysis	
SYS-7	High	OBJ-1	The thrust stand shall have an accuracy of 10 μN	Analysis	
SYS-8	High	OBJ-1	The thrust stand shall have adjustable components to accommodate various different thrusters	Demonstration	
Leveling System Requirements					
LVL-1	High	OBJ-1	The leveling system shall be able to level the thrust stand with fine adjustments	Demonstration	
LVL-2	High	OBJ-1	The levelness of thrust stand can be monitored outside of the vacuum chamber	Demonstration	
Flexure and Optical Sensing System Requirements					
FOP-1	High	SYS-6, SYS-7	Optical Sensor shall be able to detect linear displacement with high accuracy and precision.	Demonstration	
FOP-2	High	OBJ-1	Optical Sensor shall be able to report back time-stamped displacement data with accurate data collection in terms of thousands of an inch for precision	Demonstration	
FOP-3	High	SYS-7	Flexure Pitvots shall be able to allow axial rotation at a known spring constant of 3.2610 to allow ~1.0 degrees of rotation	Analysis	
Damping System Requirements					
DMP-1	Low	SYS-4	The damping system strength will be adjustable from outside the vacuum chamber	Demonstration	
DMP-2	Medium	SYS-7	The damping system will have a damping ratio of: $0.4 < \zeta < 0.8$	Analysis	

Figure A.2: Requirements Verification Matrix

A.2 Leveling System Full Characteristics

Name	Vendor	Cost	Travel Distance	Max Load Capacity	Requirements	Req Cost	Link
Vacuum-Compatible Piezo Inertia Actuator	Thorlabs	$795.00	10 mm	30 N	KIM101 Controller and Power Supply	$1,094.14	ww.thorl
Vacuum Compatible Motorized DC Servo Actuator	Thorlabs	$926.29	6mm - 25mm	9 kg	K Cube Brushed DC Servo Motor Controlle	2x$677.41	ww.thorl
Picomotor Actuator, Vacuum Compatible	Newport	$899	12.7 mm	22 N	Driver	$717	ww.new
N-111 OEM Linear Vacuum Actuator PiezoWalk	PI	Quote	10 mm	50 N gen, 70 N Hold	Digital Motion Controller	Quote	ww.pi-
Non-Motorized							
Name	**Vendor**	**Cost**	**Travel Distance**	**Max Load Capacity**	**Requirements**	**Req Cost**	**Link**
Vernier Micrometer	Newport	$87	13 mm	9 lb	None	N/A	ww.new
Vernier Micrometer	Newport	$135	25 mm	23 lb or 102ish N	None	N/A	https://w
Micrometer Head	GPM	Quote	25 mm	Unk	None	N/A	https://h

A.3 Micrometer Bracket Machine Drawing

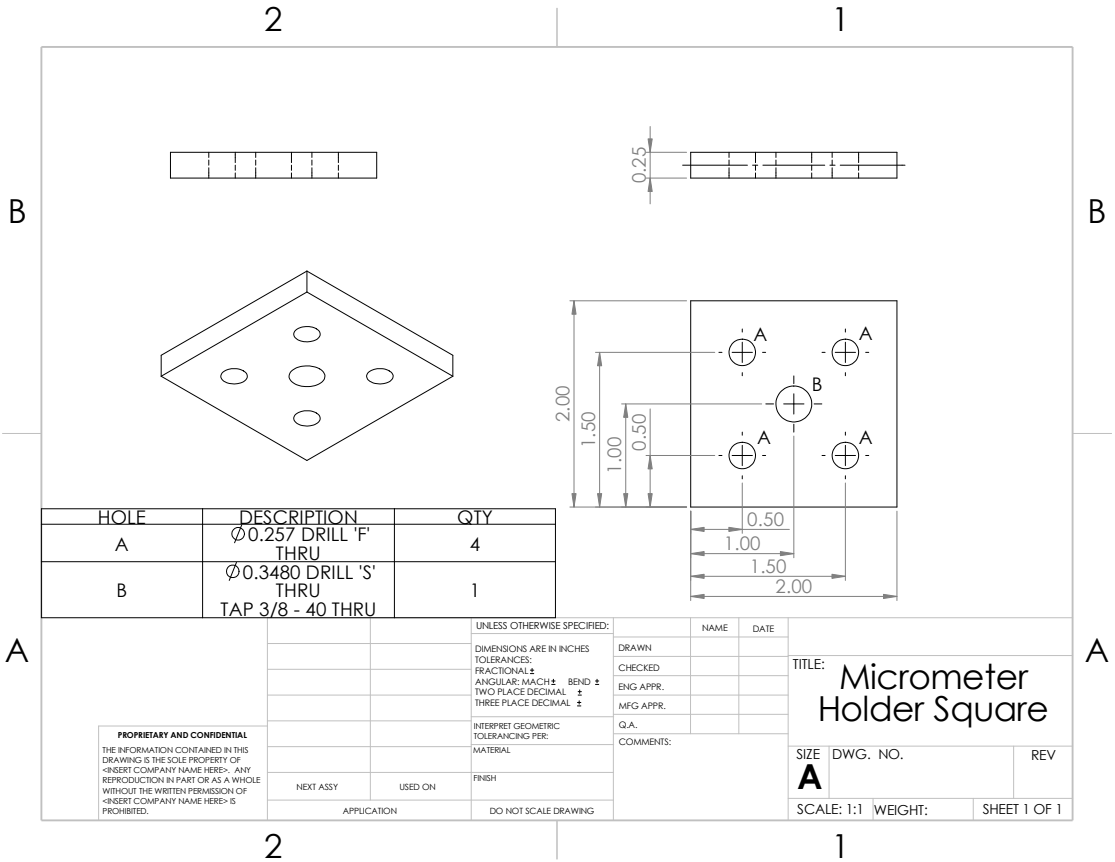

A.4 V-Channel Machine Drawing

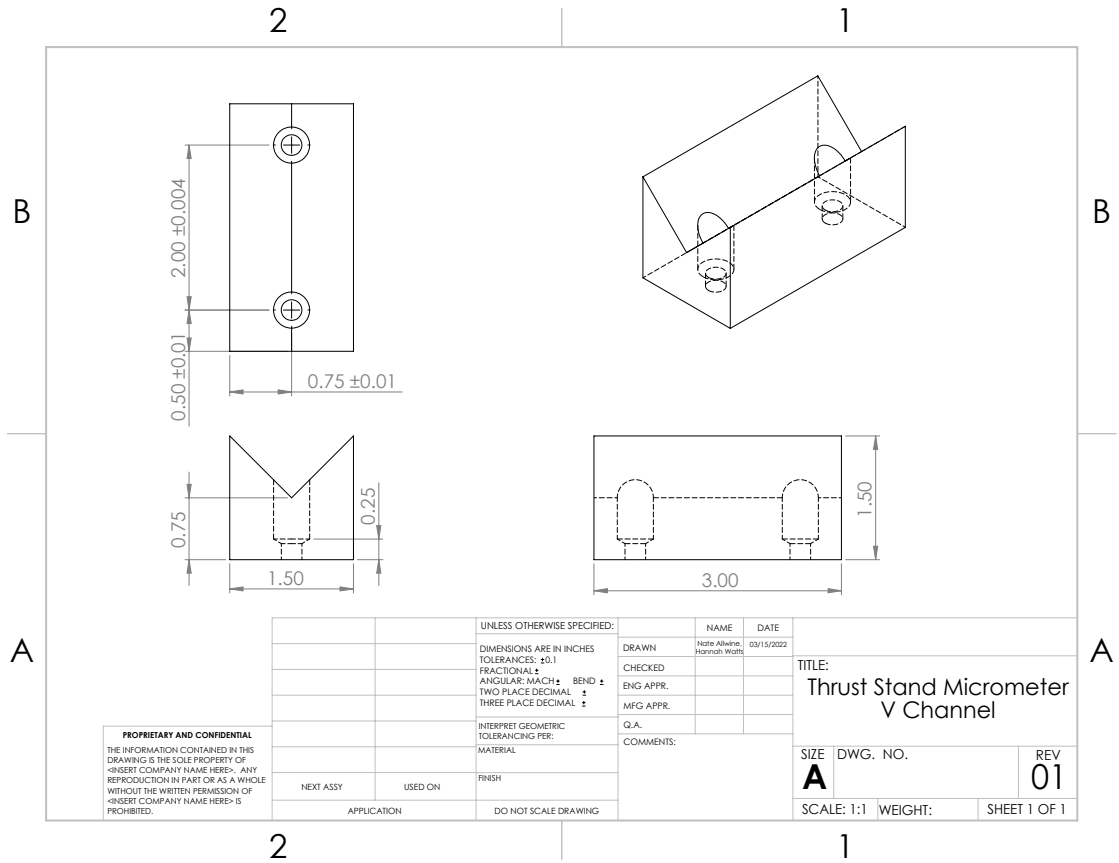

A.5 ADIS16209 Code

```
/*Register Address Available
 * 0x0400 XAccleration_out
 * 0x0600 YAccleration_out
 * 0x0A00 Temperature_out
 * 0x0C00 Xinclination_out
 * 0x0E00 Yinclination_out
 * 0x1000 Rotation_out
 */

#include <SPI.h>
const int slaveSelect = 5; //slave select pin is set to 5 digital on arduino


void setup() {
  pinMode(slaveSelect, OUTPUT); //slaveselect pin 5 is set to output mode
  SPI.begin(slaveSelect); //starts SPI for slave 1
  Serial.begin(9600); //starts arduino serial to readout values
}

void loop() {
  Serial.println("Starting data collection: "); //debuging text into serial
  SPI.beginTransaction(SPISettings(1000000, MSBFIRST, SPI_MODE3));  //initialize
spi settings
  digitalWrite(slaveSelect, LOW); //set slaveselect to low so  slave 1 listens
  uint16_t prodID1 = SPI.transfer16(slaveSelect, 0x4A00); //send 16 bit message to
slave 1 to send back product ID (Used for verifying SPI connection default response
is 0x3F51)
  digitalWrite(slaveSelect, HIGH); //set slaveselect to high so slave 1 stops
listening
  //Serial.print(prodID1, BIN); //prints out the response from slave 1
  Serial.println("");
  delay(1000); //delay for a second (Unnessassary)
  SPI.endTransaction(); //ends the SPI transaction
}
```

```
/*Register Address Available
 * 0x0400 XAccleration_out
 * 0x0600 YAccleration_out
 * 0x0A00 Temperature_out
 * 0x0C00 Xinclination_out
 * 0x0E00 Yinclination_out
 * 0x1000 Rotation_out
 */

#include <SPI.h>
const int slaveSelect = 5; //slave select pin is set to 5 digital on arduino


void setup() {
  pinMode(slaveSelect, OUTPUT); //slaveselect pin 5 is set to output mode
  SPI.begin(slaveSelect); //starts SPI for slave 1
  Serial.begin(9600); //starts arduino serial to readout values
}

void loop() {
  Serial.println("Starting data collection: "); //debuging text into serial
  SPI.beginTransaction(SPISettings(1000000, MSBFIRST, SPI_MODE3));  //initialize
spi settings
  digitalWrite(slaveSelect, LOW); //set slaveselect to low so  slave 1 listens
  //uint16_t prodID1 = SPI.transfer16(slaveSelect, 0x4A00); //send 16 bit message to
slave 1 to send back product ID (Used for verifying SPI connection default response
is 0x3F51)
  uint16_t xinc1 = SPI.transfer16(slaveSelect, 0x0C00); //xinc command and response
  Serial.print(xinc1, BIN); //prints out the response from slave 1
 Serial.print(xincdeg);
 Serial.println("");
  delay(1000); //delay for a second (Unnessassary)
  SPI.endTransaction(); //ends the SPI transaction
}
```

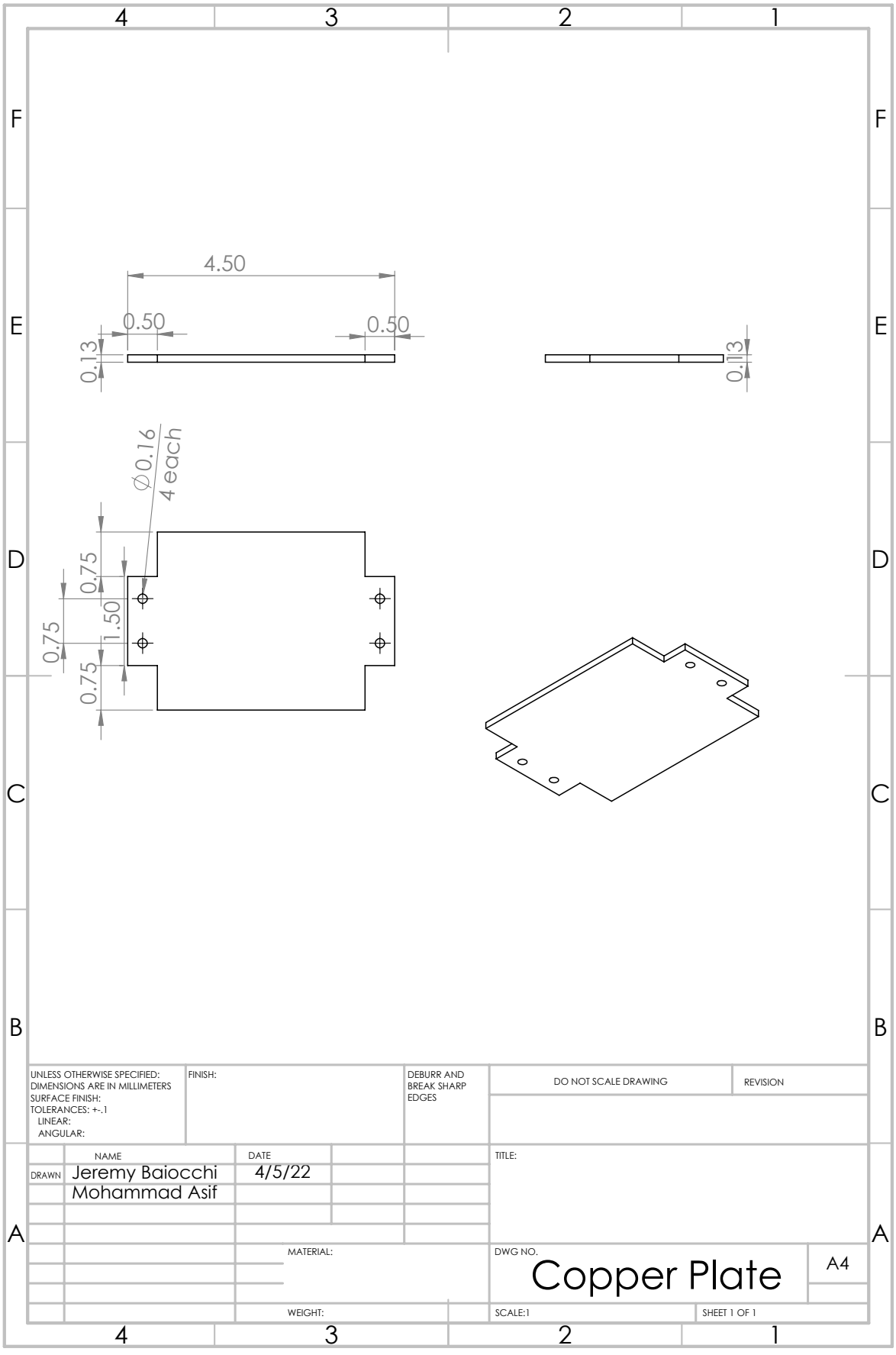
4.50
0.50
0.50
0.13
0.13
Ø0.16
4 each
0.75
1.50
0.75
0.75
UNLESS OTHERWISE SPECIFIED:
DIMENSIONS ARE IN MILLIMETERS
SURFACE FINISH:
TOLERANCES: +-.1
LINEAR:
ANGULAR:
FINISH:
DEBURR AND BREAK SHARP EDGES
DO NOT SCALE DRAWING
REVISION
NAME
DATE
DRAWN
Jeremy Baiocchi
Mohammad Asif
4/5/22
TITLE:
MATERIAL:
DWG NO.
Copper Plate
A4
WEIGHT:
SCALE:1
SHEET 1 OF 1

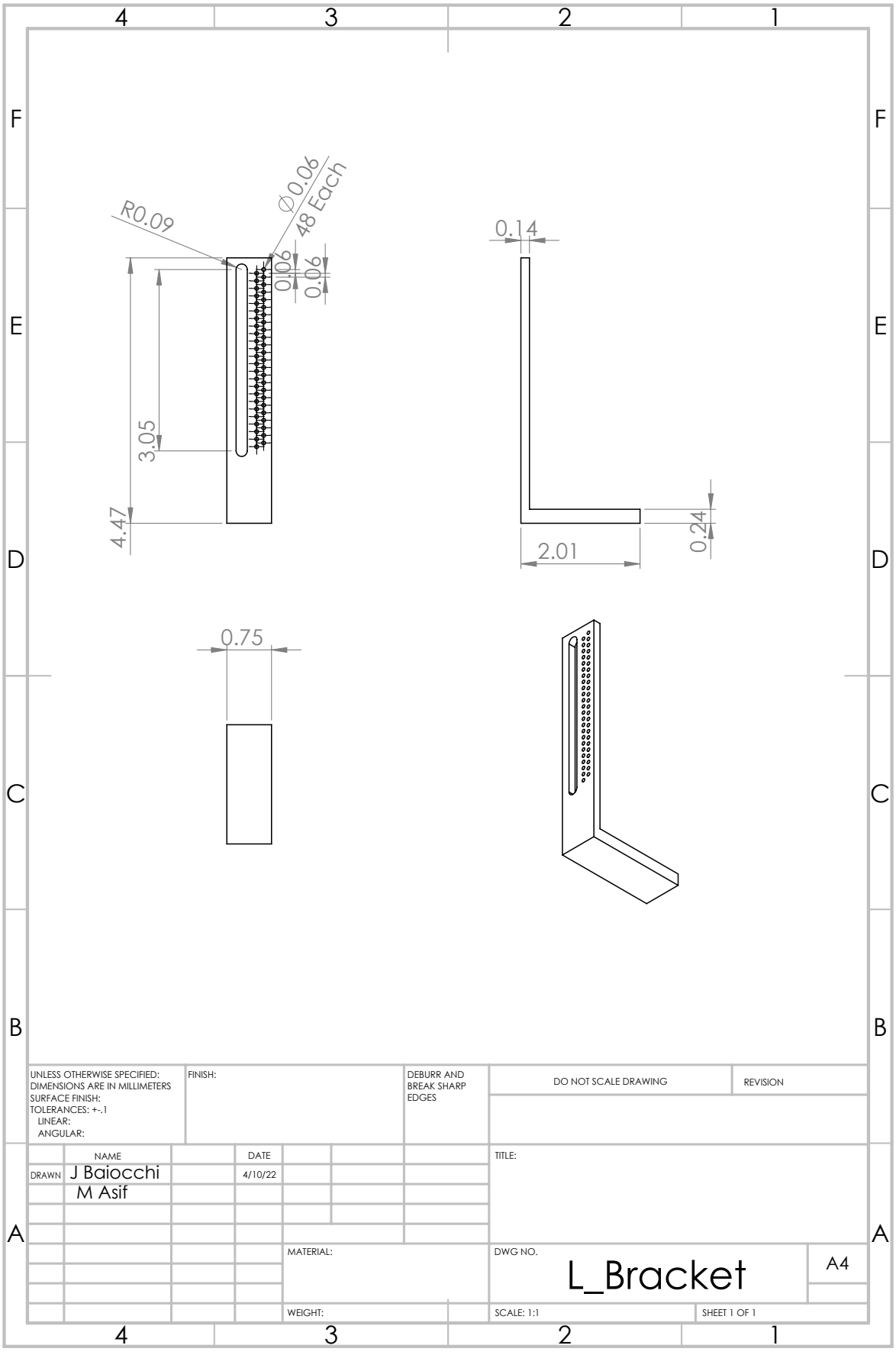
4
3
2
1
F
E
D
C
B
A
R0.09
Ø0.06
48 Each
0.06
0.6
3.05
4.47
0.14
0.24
2.01
0.75
UNLESS OTHERWISE SPECIFIED:
DIMENSIONS ARE IN MILLIMETERS
SURFACE FINISH:
TOLERANCES: +-.1
LINEAR:
ANGULAR:
FINISH:
DEBURR AND BREAK SHARP EDGES
DO NOT SCALE DRAWING
REVISION
NAME
DATE
DRAWN
J Baiocchi
M Asif
4/10/22
TITLE:
MATERIAL:
DWG NO.
L_Bracket
A4
WEIGHT:
SCALE: 1:1
SHEET 1 OF 1

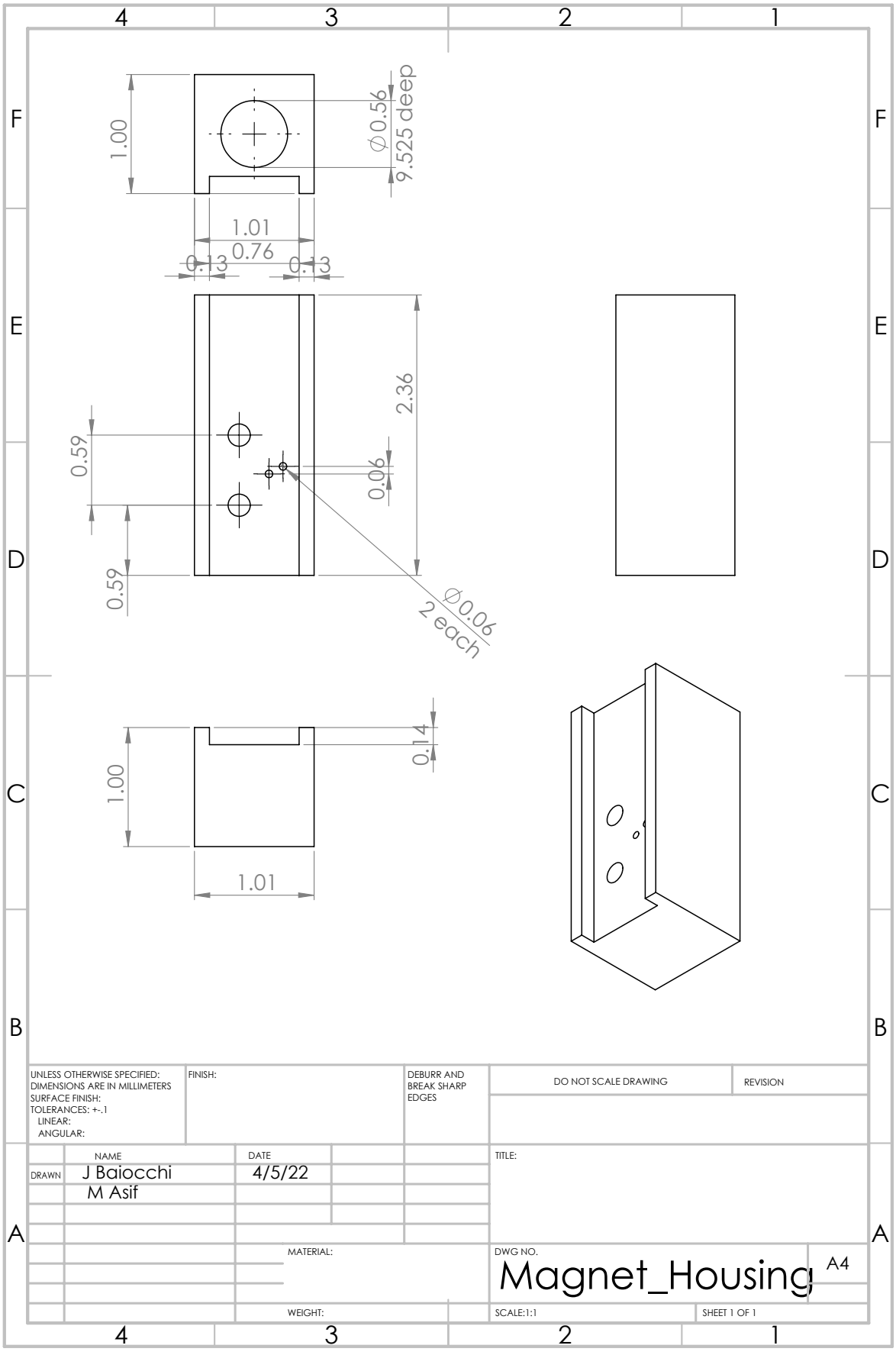
4
3
2
1
F
E
D
C
B
A
1.00
⌀0.56
9.525 deep
1.01
0.76
0.13
0.13
2.36
0.59
0.06
0.59
⌀0.06
2 each
0.14
1.00
1.01
UNLESS OTHERWISE SPECIFIED:
DIMENSIONS ARE IN MILLIMETERS
SURFACE FINISH:
TOLERANCES: +-.1
LINEAR:
ANGULAR:
FINISH:
DEBURR AND BREAK SHARP EDGES
DO NOT SCALE DRAWING
REVISION
NAME
DATE
DRAWN
J Baiocchi
M Asif
4/5/22
TITLE:
MATERIAL:
DWG NO.
Magnet_Housing
A4
WEIGHT:
SCALE:1:1
SHEET 1 OF 1

A.6 ABET Program Evaluation Questionnaire

See below for ABET Program Evaluation Questionnaire Mechanical and Aerospace Engineering Project (ME/AE 4800) Program Outcomes' Indicators Assessment Worksheet Mechanical and Aerospace Engineering Programs

ABET Program Evaluation Questionnaire
Mechanical and Aerospace Engineering Project (ME/AE 4800) Program Outcomes' Indicators Assessment Worksheet
Mechanical and Aerospace Engineering Programs

Semester: Spring 2022 Project Group Number: 04-22-13

Project Title: **Design, Optimization, and Construction of Flexure, Optical, Damping, and Leveling Systems for Electric Propulsion Thrust Stand**

Student Team Members: **Nathaniel Allwine, Jeremy Baiocchi, Logan Hefferan**

Faculty Team Members: **Dr. Kristina Lemmer**

Please respond to all of the following questionnaires as best you can.

Outcome (2) An ability to apply engineering design to produce solutions that meet specified needs with consideration of public health, safety, and welfare, as well as global, cultural, social, environmental, and economic factors.

Performance Indicators:

1. Generates a detailed statement of all the specified engineering needs for the design project.
2. Identifies and lists potential public health, safety and welfare concerns for consideration in the design process.
3. Identifies and lists global, cultural, social, environmental and economic factors that are relevant to the development of the project product.
4. Produces solutions that satisfy the engineering needs, address the public concerns and consider the effects of the relevant design factors.

(If you copy and paste from the report, mention Section number or page numbers. If any question or item is not relevant to your project, write N/A)

Performance Indicator 1

Describe the engineering needs for this project.

Western Michigan University is host to three organizations that work with electric propulsion thrusters currently without a way of obtaining direct experimental thrust data.

List the project goals along with performance criteria.

The flexure, optical sensing, damping and leveling systems for a thrust stand originally designed by Hannah Watts in her WMU Honors Thesis: Design of A Thrust Stand for Electric Propulsion will be completed. These systems will be redesigned, optimized, and finally constructed to be integrated into the thrust stand structure.

List the project constraints.

- **Timeline: contribute to thrust stand development in a timely manner so WMU SWARM-EX has a working thrust stand before thruster development has concluded**
- **Environment: Entire stand must fit within the ALPE high-vacuum chamber so that it can be utilized for testing while also utilizing only vacuum-rated materials**
- **Cost: developing these systems well within the NSF provided budget so that the project can be finished**
- **Precision and Accuracy: The final product must be able to be utilized for incredibly small thrust increments since electric propulsion thrusters operate on the scale of micro-Newtons.**

List the methods/procedures that were implemented to ensure that the customer expectations were addressed.

- **Established clear object statements with completion criteria.**
- **Documented system requirements and constraints for operation in vacuum environment.**
- **Recorded approximate thrust values for various thruster to determine measurement range of thrust stand and ensure subsystems would meet this requirement.**

Performance Indicator 2

Describe potential public health, safety, and welfare concerns regarding this project and describe how they were addressed in the final design.

Public health: **The completed thrust stand may be difficult to load and unload from the vacuum chamber without assistance from another member due to its uneven weight distribution.**

Public safety: **Electric propulsion thrusters do not operate outside of a vacuum environment. Any ion, plasma, or gas emission will be contained within the vacuum chamber.**

Public welfare: **N/A**

Performance Indicator 3

List and explain all possible global, cultural, social, environmental, and economic factors relevant to the product of this project.

Global factors: **N/A**

Cultural factors: **N/A**

Social factors: **The proposed thrust stand systems will include documentation and low-cost options wherever possible to allow for other electric propulsion teams to replicate the design for their own use.**

Environmental factors: **N/A**

Economic factors: **Keeping cost low is important to reduce the barrier of entry to electric propulsion thruster analysis.**

Performance Indicator 4
(To be addressed by the faculty adviser).

Outcome (5) An ability to function effectively on a team whose members together provide leadership, create a collaborative and inclusive environment, establish goals, plan tasks and meet objectives

Performance Indicators:

1. Student's ability to function effectively
2. Student provides task specific leadership.
3. Student creates a collaborative and inclusive environment.
4. Group establishes goals.
5. Group plans tasks
6. Group meets objectives.

(If you copy and paste from the report, mention Section number or page numbers.)

Performance Indicators 2 & 5
List all tasks required to accomplish the goals of this project, and name the group member responsible for the completion of each task.

Nathaniel Allwine was required to design, construct, and test the leveling system for the thrust stand.
Logan Hefferan was required to design, construct, and test the optical and flexure system.
Jeremy Baiocchi was required to design, construct, and test the damping system.

Performance Indicator 1
(Project's adviser will determine whether the listed tasks were completed).

Every student must answer the following question (add Student 3 & 4 if needed):

Student 1 name: Nathaniel Allwine
For project tasks in which I was **not** the leader, I provided the following inputs towards their completion:

Helped with brainstorming sessions for any problem that might arise. Provided advice for situations in which I might've had more experience.

Student 2 name: Jeremy Baiocchi
For project tasks in which I was **not** the leader, I provided the following inputs towards their completion:

Budget discussion and allocation. Concept brainstorming for system design, integration, and interaction.

Student 3 name: Logan Hefferan
For project tasks in which I was **not** the leader, I provided the following inputs towards their completion:

Various solution concepts and brainstorming regarding thermal dissipation of an electromagnet.

Performance Indicator 3
For project tasks in which you **were** the leader, describe the input other group members provided towards the successful completion of these tasks.

Student 1: Nathaniel Allwine

The other group members provided estimated budgets for their systems and helped determine level of importance for their systems which allowed me to make decisions to go with more cost-effective solutions.

Student 2: Jeremy Baiocchi

Provided knowledge of vacuum chamber operations, machining assistance/instruction, and extra pairs of hands during testing and documentation work. Additionally provided common sense theory and dimension checks along the way to stay on track.

Student 3: Logan Hefferan

Expertise in the integration of respective systems and the interactions each would produce in regards to my system. Physical positioning and fastening of each system in a manner that allowed considerations of different strength and different size equipment to allow proper interaction of cross-system components.

Performance Indicator 4
List all goals this project had to satisfy to be considered successfully completed.

Completed leveling, flexure, optical, and damping systems to be integrated into thrust stand.

Performance Indicator 6
(To be addressed by the faculty adviser).

Outcome (7) An ability to acquire and apply new knowledge as needed, using appropriate learning strategies.

Performance Indicators:

1. Student's ability to find information relevant to problem solution without guidance.
2. Student's ability to identify the additional knowledge needed to complete project.
3. Student's ability to acquire and apply the additional knowledge needed to complete project.

Performance Indicator 1

Describe what information you found in order to successfully complete the tasks you were assigned in the project.

Student 1: Nathaniel Allwine

I found examples of existing thrust stands used for electric propulsion and determined the methods they used for leveling. Additionally, I found component information for certain leveling mechanisms to determine which would be best for the system. Research was also done on SPI serial communication and the leveling sensor that was purchased to read the output properly.

Student 2: Jeremy Baiocchi

Researched existing damping solutions and determined which would provide best performance and adjustability. Designed, tested, and integrated multiple potential solutions for damping system. Provided clear path for future work to continue to improve damping system.

Student 3: Logan Hefferan

Used information found from other thrust stand projects to determine in what different manners displacement was measured so that multiple options could be considered. Additionally, access supplier websites to determine which displacement sensors were most appropriate for this application based on the specifications of each product.

What sources did you use to find this information?

Student 1: Nathaniel Allwine

I used academic journals and articles. Additionally, I used company websites to find manuals and users guides on their components.

Student 2: Jeremy Baiocchi

I relied heavily on academic journals and existing thrust stand documentation.

Student 3: Logan Hefferan

I used the websites of the suppliers to access all the product specifications pertaining to this application. Also on these sites, I was able to access basic software setups and equipment user manuals to learn how to use the optical sensor properly. I also used academic journals to see how other groups measured displacement.

Performance Indicator 2

Describe what additional knowledge/skills you needed to acquire or improve in order to successfully complete the tasks you were assigned in the project.

Student 1: Nathaniel Allwine

I learned about SPI serial communication and how to use it to communicate with devices. I also learned how to do machining in order to make in house parts.

Student 2: Jeremy Baiocchi

I watched and researched several online lectures that taught me how to use Matlab and Comsol magnetic modeling suites. I learned how to spot weld a thermocouple. I improved my CAD modeling abilities using new-to-me software.

Student 3: Logan Hefferan

Performance Indicator 3

Describe what approach/process you followed in order to acquire or improve the additional knowledge/skills you needed.

Student 1: Nathaniel Allwine

I would reach out to an expert in the field and ask if they would be willing to show me simple steps be able to learn the skills. The internet was also a common resource for me to quickly find simple answers about trivial things I might not know about.

Student 2: Jeremy Baiocchi

Matlab and Comsol have excellent documentation on how to interact and retrieve data from simulations. Everything I need was able to be found by digging through their online libraries. For other issues talented members within the team were able to point me in the right direction for assistance.

Student 3: Logan Hefferan

The internet was used to learn about the basic physical principles about the products of interest. If necessary, I would often reach out to the suppliers that produce these products to gain more in-depth information.

A.7 Resumes

Nathaniel Allwine

nathaniel.j.allwine@wmich.edu · (269) 329-9533

I'm a highly motivated aerospace engineering student currently attending Western Michigan University with experience in leadership and team building.

Education

Western Michigan University — Kalamazoo, Michigan
BS Aerospace Engineering expected 2022 — Sep 2018 - Current

- GPA: 3.75/4.0
- Member of Lee Honors College
- Member of Alpha Lambda Delta Honors Society

Educational Experience

Western Aerospace Launch Initiative (WALI) — September 2018 - Current
Co-Chief Engineer 2021 - Current

- Compose and review documentation submitted to review board
- Lead team through meetings and tasks

Payload Team Member 2018 - 2021

- Tasked with testing and documenting the payload systems for cube satellite
- Designed LED array to replicate Teflon spectrum from Pulsed Plasma Thruster (PPT)
- Designed and documented testing procedure for in house plasma diagnostics with Langmuir probe
- Wrote scripts for testing and data processing for a Langmuir probe

Aerospace Laboratory for Plasma Experiments (ALPE) — October 2019 - Current
Student Assistant

- Vacuum chamber experimental setup, provided testing assistance, laboratory organization and upkeep

SWARM-EX CubeSat Team — May 2021 - Current
Propulsion Team Member

- Integrated and documented electrical components into thrust stand design for low thrust propulsion systems

Advanced Rocketry Club (ARC) — September 2018 - Current
Chief Engineer 2020 - Current

- Lead team through meetings and tasks
- Designed and produced a CAD model of entire payload system
- Assembled, tested, and documented GPS system
- Participating in Argonia Cup Collegiate Rocketry Competition

Payload Team Member 2018 - 2020

- Responsible for designing, testing and documenting the mission payload system
- Participated in NASA SLI Competition and Argonia Cup Collegiate Rocketry Competition
- Developed Arduino based payload parachute GPS guidance system

Professional Experience

Pro Services — Portage, Michigan
Project Manager Intern — November 2020 - Present

- Designed and implemented system for daily and long term project progression reporting and worker productivity
- Site-wide inspection of components with isometric and P&ID drawings to provide quality assurance and completion status

Relevant Skills

- Microsoft Excel, Powerpoint, AutoCAD, Inventor, LabView, Matlab, Navisworks, and SolidWorks
- C, C++, Java, ReactJS, and Python

Jeremy Baiocchi
jeremy.baiocchi@wmich.edu · (708) 601-2321

Education

Western Michigan University — Kalamazoo, Michigan
Bachelor of Science — April 2022
Major: Aerospace Engineering
Minor: Mathematics
GPA: 3.50
Dean's List: 6 semesters

Texas State Technical College - West Texas — Abilene, Texas
FAST Trac Airframe and Powerplant Technician Program — Spring 2018
Curricula focused on linking military/civilian skills, training, and regulations

Work Experience

Duncan Aviation BTL — Battle Creek, Michigan
Turbine Engine Technician 3 — March 2019 - Present
- Perform troubleshooting, repair, and other general maintenance of aircraft engines, systems and components
- Execute various scheduled inspections on a variety of business class aircraft
- Manufacturer experience: Pratt & Whitney, Rolls-Royce, GE, Honeywell, and Williams

Fixed Base Operator (FBO) Customer Service Representative — September 2018 - March 2019
- Liaison between customers and company service members
- Fulfilled requests from customers, vendors, and team members
- Supervised aircraft movement and fueling operations

United States Air Force — Dyess AFB, Texas
B-1B Aircraft Technician — August 2012 - August 2018
- Non-commissioned officer
- Achieved skill rating of *Craftsman* (7 level)
- Supervised launch, recovery, and ground movement operations of aircraft
- Trained personnel on maintenance procedures and safety policies
- Performed various aircraft inspections and documented/repaired discrepancies

Skills/Certifications

- Federal Aviation Administration (FAA) Airframe and Powerplant Certificate
- Federal Secret security clearance (inactive 2018)
- Airman Leadership School - selected for participation in a 240 hour leadership mentoring program
- Experience with Microsoft Office, Google Workspace, LaTeX, MATLAB, Java, and Python
- Forklift Operator
- Heavy crane operator (24 Ton)
- Communication, leadership, problem solving, and troubleshooting
- Precise documentation of aircraft logbooks

References

- Available upon request

Logan S. Hefferan

2453 Kingscross Drive, Shelby Township, MI 48316 | (248) 978-8051
logan.s.hefferan@gmail.com | logan.s.hefferan@wmich.edu

Seeking permanent employment to utilize and exercise my skills and abilities in a manner which aids the team's mission. Additionally, to address engineering issues and solve complex problems using said engineering skills.

Work Experience

Production Engineering Intern
DEVCOM Ground Vehicle System Center – U.S. ARMY
May 2021 – August 2021 (40 hours/week)
Supported Industrial Engineers in the Stryker Brigade Combat Team to address production-related engineering issues and new Stryker Combat Vehicle engineering projects. Cooperated with General Dynamics and Oshkosh Defense contractors.

Equipment Engineering Intern
Tesla Inc. – Fremont Factory
January 2020 – April 2020 (40+ hours/week)
Required the use of CATIA, Project Management, and Excel to improve OEE and Production, while reducing downtime and CPU in the Body Paint Shop for the Models S, X, 3, and Y.

Process Engineering Intern
Tesla Inc. – Fremont Factory
September 2019 – December 2019 (40+ hours/week)
Required the use of Excel, CATIA, process development, and statistical analysis to solve problems across cross-functional groups throughout the plant. Goals focused on the successful painting and production of the Models S, X, 3, and Y.

Manufacturing/Production Intern
Fiat Chrysler Automobiles – Sterling Heights Assembly Plant
May 2019 – August 2019 (40+ hours/week)
Required the ability to solve problems and production issues to maintain a high volume and quality of production of the painted cabs for the RAM 1500. Responsible for leading and supervising up to 40 production operators.

Education

Western Michigan University, **BSE Aerospace Engineering**
Minor: **Mathematics**
Expected Graduation Date: **April 30, 2022**
Senior | GPA: ***3.57***

- 2017 WMU Medallion Scholar
- Lee's Honors College and Dean's List
- Senior Engineering Design Project: *Design, Optimization, and Construction of Flexure, Damping, and Leveling Systems for Electric Propulsion Thrust Stand*

Skills & Certifications

- Skilled in AutoCAD, SolidWorks, Inventor, CATIA, Windchill Software, and GD&T knowledge
- Process Development, OEE, Cost Optimization/LEAN
- Standard Instructions, SOP Writing, and Contract Review
- MATLAB, C, C++, Java, and LabVIEW experience
- MODAPTS Certified
- Skilled in Microsoft Office
- Leadership, Project Management, and Teamwork Skills

Activities & Leadership

- AIAA Pegasus Student Chapter
  - President, Rocketry Team Member
- Tau Beta Pi Engineering Honor Society
- Alpha Lambda Delta Honor Society
- Western Student Association
  - AIAA Student Representative
- WMU Running Club
  - VP, Secretary, Event/Travel Coordinator